Thermal Lens Spectroscopy

Mladen Franko
Laboratory of Environmental Research, University of Nova Gorica, Nova Gorica, Slovenia

Chieu D. Tran
Department of Chemistry, Marquette University, Milwaukee, WI, USA

The thermal lens technique is based on measurement of the temperature rise that is produced in an illuminated sample as a result of nonradiative relaxation of the energy absorbed from a laser. Because the technique is based on direct measurement of the absorbed optical energy, its sensitivity is higher than conventional absorption techniques. However, advantages of the thermal lens technique are not only limited to its ultrasensitivity but also include other unique characteristics including small-volume sample capability and dependency on thermo-optical properties of solvents. In this overview, the theory of the technique is initially described. The main focus is, however, on the instrumentation and applications based on unique characteristics of the technique. Specifically, the discussion begins with a description of different types of thermal lens apparatuses (e.g. single-beam and double-beam instruments, differential, multiwavelength, thermal lens-circular dichroism instruments, and thermal lens microscope). A detailed description of various applications including applications based on its ultratrasensitivity (e.g. applications in environment, agriculture and food science, biochemistry and biomedicine, measurements in the near- and middle-infrared region, and kinetic determination), applications based on its small-volume capability (microfluidic devices, detection for capillary electrophoresis), and applications based on exploitation of its dependency on thermal physical properties of solvents to either determine physical properties of the solvent or to further enhance the sensitivity of the technique follows. Finally, the future of the technique is forecasted.

1 INTRODUCTION

The availability of lasers makes it possible to observe and measure a variety of phenomena, which would not otherwise be feasible using other light sources. One such phenomenon is the photothermal effect.[1] In the case of the thermal lens,[1–10] which is a type of photothermal effect, a sample is excited by a laser beam, which has a symmetrical intensity distribution (TEM_{oo}). The nonradiative relaxation releases the absorbed energy in the form of heat. The heat generated is strongest at the center of the beam because the beam intensity is strongest at that point. Consequently, a lenslike optical element is formed in the sample owing to the temperature gradient between the center of the beam and the bulk material. The thermal lens effect is observable for laser beams in the power range of only microwatts in samples normally thought to be transparent, and is thus suitable for the low-absorption measurement of nonfluorescent samples. Its sensitivity is relatively higher than that of the conventional transmission or reflection measurements because, in this technique, the absorbed energy is measured directly.

The first measurement of the thermal lens effect was performed by Gordon et al. in 1965 using a simple single-beam apparatus.[1] Theories have since been derived to explain the effect and to facilitate its applications to chemical analyses and characterization. Experimentally, recent advances in optics, electronics,

Encyclopedia of Analytical Chemistry R.A. Meyers (Ed.)

quantum electronics, and material science have been synergistically exploited to develop novel instruments that have lower background noise, higher sensitivity and selectivity, and wider applications (by expanding its measurement capability from the conventional visible region to the ultraviolet, near-infrared, and infrared regions). The unique characteristics of lasers, namely low-beam divergence, pure polarization, high spectral and spatial resolution, and its ability to be focussed to a diffraction-limited spot, have been fully exploited to use the thermal lens as a detection technique for microfluidic devices. As a consequence of these developments, the thermal lens technique has been established as a highly sensitive technique for trace chemical characterization, including single molecule detection.

In addition to its ultrasensitive and small-volume capabilities, the thermal lens technique has other features that cannot be rivalled by other techniques namely, the thermal lens signal is dependent not only on sample concentration and excitation laser power but also on the position and thermophysical properties of the sample. These unique features have been exploited either to further increase its sensitivity or to use it for sensitive and accurate determination of thermal physical properties of a variety of substances including solids, liquids, and gases.

Owing to its advantages and unique features, the thermal lens technique has been extensively reviewed.[2–10] However, most of these reviews are restricted to relatively narrow topics and/or applications (e.g. instrumentation, applications in separations, agriculture, environmental, and microfluidics) or are a part of a broader topic such as photothermal techniques, which include not only the thermal lens techniques but also photothermal deflection, photopyroelectric, photothermal interferometry, as well as photoacoustic spectroscopy.

This review is written as a self-contained, standalone article on the thermal lens technique. It is not only intended for analytical spectroscopists who are knowledgeable in this field but also for readers who are not specialists on this topic. To accomplish this goal, the first part of this review is a theoretical treatment of the technique to provide a fundamental understanding of this approach as well as to enable readers to follow discussion in the subsequent chapter on instrumentation. Various types of thermal lens apparatuses are discussed in detail in chronological order, commencing with the historical single-beam instrument developed by Gordon back in 1965, and ending with microfludics and near-field devices with multiwavelength capability. Subsequent sections are devoted to applications based on unique features and capabilities of the thermal lens technique, primarily its ultrasensitivity (applications in chemistry, biochemistry and medical science, agriculture and foods, environment, and reaction kinetics), its small-volume capability (microfluidic devices, capillary electrophoresis), its use for the determination of thermal physical properties, and methods based on its dependency on thermo-optical properties of sample matrix to enhance its sensitivity. Finally, possible future aspects of the technique are also discussed.

Finally, it is important to emphasize that this article is restricted to the thermal lens technique, which is one of the many photothermal techniques. Others include photothermal beam deflection, photoacoustic spectroscopy, photothermal interferometry, and photopyroelectric techniques. Reviews on these other techniques may be found elsewhere in the literature.[2–4,6]

2 THEORY

It is generally accepted that the thermal lens effect originates from nonradiative relaxation of excited species in a sample irradiated by a laser beam with a Gaussian intensity profile. During such radiationless relaxation processes, which include vibrational relaxation, intersystem crossing, and external conversion, the absorbed energy from the excitation light is converted to heat. As a result, the temperature of the irradiated sample changes and a refractive index gradient is formed in the sample, resulting in a change in the laser beam radius, and a related change in the intensity of the beam on its axis. The magnitude of the thermal lens effect is proportional to the amount of heat generated in the irradiated sample, and is consequently dependent on the power P of the excitation light, absorbance A of the sample, as well as on the fluorescence efficiency of absorbing species, which decreases the thermal lens effect. Thermo-optical properties of the medium (i.e. temperature coefficient of refractive index – $\partial n/\partial T$ and thermal diffusivity $D = k/\rho c_p$, where k, ρ, and c_p represent thermal conductivity, density, and heat capacity, respectively) also have an important impact on the magnitude of the thermal lens effect.

Different theoretical descriptions of the thermal lens effect under a variety of experimental conditions can be found in the literature and have been reviewed extensively in several books and review articles.[6–8,11–14] These models cover thermal lens effects generated under pulsed and continuous wave (CW) excitation, and under different pump/probe geometries, i.e. single and dual beams as well as collinear and crossed-beam configurations. Furthermore, steady and flowing sample conditions have been considered.

For illustration, the thermal lens theory for a collinear thermal lens experiment is presented, starting from one of the most general thermal lens theories introduced by Gupta,[13] which can be used to describe the thermal lens

effect under various possible experimental conditions. This approach accounts for different pump–probe geometries and type of excitation beam (pulsed and CW), and optical configuration of pump and probe beam, as well as the effects of heat loss in flowing systems. All of these variations must be accounted for when solving the nonsteady thermal diffusion equation appropriate for this problem:

$$\frac{\partial T(r,t)}{\partial t} - D\nabla^2 T(r,t) - v_x \frac{\partial T(r,t)}{\partial x} + \frac{1}{\rho C_t} Q(r,t) \quad (1)$$

where $T(r,t)$ is the temperature change at time t, in a sample with a uniform velocity v_x in direction x (perpendicular to the axis of excitation beam). The parameter $Q(r,t)$ is the source term. It represents the heat produced in unit time per unit volume of the sample due to the absorption of excitation light and subsequent radiationless deexcitation of excited atoms or molecules in the sample. The source term depends primarily on the mode of excitation and other experimental parameters. These dependencies can be written in simplified forms if the sample is presumed to be optically thin (transmittance ≈ 1), which is usually the case in thermal lens measurements. Another assumption is that the concentration of absorbing species remains constant during the excitation. The solution to the thermal diffusion equation gives the time-dependent temperature rise inside the sample and enables calculation of the refractive index gradient, which acts upon the laser beam as an optical element, i.e. the thermal lens. The relative change in the intensity of the light on the probe beam axis, measured in the far field, is generally known as the ''thermal lens signal'' (S), which for the given case and for a periodic pump beam modulation at angular frequency $\omega_m = 2\pi f$ (in such case $Q(r,t) = (2.303\alpha P/\pi a^2)\ (\exp(-2(x^2+y^2)/a^2))(1+\cos\omega_m t)$) can be written as follows:

$$S(t) = -4\frac{2.303PAz_1}{\pi\rho c_p}\left(\frac{\partial n}{\partial T}\right)\int_0^t \frac{(1+\cos\omega_m\tau)}{[a^2+8D(t-\tau)]^2} \times\left[2-\frac{4[x-v_x(t-\tau)]^2}{[a^2+8D(t-\tau)}\right]e^{-2[x-v_x(t-\tau)]^2/[a^2+8D(t-\tau)]}d\tau \quad (2)$$

where α is the decadic absorption coefficient of the sample, z_1 is the distance between the position of the sample and the probe beam waist, and a is the radius of the excitation laser beam. For a nonflowing sample ($v_x = 0$) and for a nonmodulated excitation beam ($\omega_m = 0$), this equation is reduced to

$$S(t) = -2\frac{2.303PAz_1}{\pi ka^2}\left(\frac{\partial n}{\partial T}\right)\frac{1}{(1+t_c/2t)} \quad (3)$$

It can then be developed further for the case where the sample is positioned one confocal distance ($z_c = \pi {a_0}^2/\lambda$) from the probe beam waist, where λ and a_0 represent the wavelength and the radius of the probe beam in its waist, respectively.

The characteristic time constant of the thermal lens is t_c. It depends on the excitation beam radius a in the sample and thermal diffusivity D, and can be expressed as

$$t_c = \frac{a^2\rho c_p}{4k} \quad (4)$$

For pump and probe beams of equal radii at confocal distance $a^2 = 2{a_0}^2$; therefore,

$$S(t) = -\frac{2.303PA}{k\lambda}\left(\frac{\partial n}{\partial T}\right)\frac{1}{(1+t_c/2t)} \quad (5)$$

This expression is identical to the one given by early theoretical models of thermal lens derived for a single-beam geometry, where one laser beam serves for excitation as well as for probing the thermal lens effect. They rely on relatively simple parabolic approximation, where the thermal lens generated by a CW excitation is treated as an ideal thin lens.[1] Such an approximation is also valid for the experimental arrangement of Gupta,[13] where the radius of pump beam is assumed to be much larger than the radius of the probe. It was already demonstrated on the basis of the earliest models that the thermal lens signal is dependent on the position of the sample relative to the laser beam waist. Maximum signal is obtained when the sample is positioned one confocal distance from the beam waist.

The parabolic model provides a good approximation of the general behavior of the thermal lens. However, the refractive index change outside the excitation area is not parabolic, and the thermal lens cannot be regarded as a thin lens. A more accurate quantitative description of the thermal lens has been given through consideration of the aberrant nature of the thermal lens, and by using diffraction theory to derive the expression for changes in laser beam intensity and related thermal lens signal,[15] i.e.

$$S(t) = -\frac{2.303PA}{k\lambda}\left(\frac{\partial n}{\partial T}\right)\tan^{-1}\left[\frac{1}{(1+t_c/t)\sqrt{3}}\right] \quad (6)$$

The so-called aberrant model of thermal lens predicts maximal signal when the sample is positioned at distance $z_1 = z_c\sqrt{3}$ from the beam waist, and demonstrates that the parabolic model overestimates the thermal lens signal by a factor of $1/\tan^{-1}(1/\sqrt{3})$. Application of the aberrant model is particularly important in dual-beam thermal lens experiments with a mode-mismatched configuration. Under such conditions, the aberrant nature of the thermal

lens is even more pronounced due to the fact that the thermal lens is generated by a pump beam focused directly inside the sample, and its beam radius a_e is usually much smaller than the radius of the probe beam a_p in the sample, which is placed at the position of maximal thermal lens ($z_1 = z_c\sqrt{3}$).

For some applications, the time dependence of the thermal lens signal is important, and based on the aberrant model the changes in probe beam intensity (I) can be expressed as

$$I(t) = I(0)\left\{1 - \theta\tan^{-1}\left(\frac{1}{(1+t_c/t)\sqrt{3}}\right) + \left[\frac{\theta}{2}\tan^{-1}\left(\frac{1}{(1+t_c/t)\sqrt{3}}\right)\right]^2 + \left[\frac{\theta}{4}\ln\left(\frac{(1+t/t_c)^2+1/3}{(2+t_c/t)^2}\right)\right]^2\right\} \quad (7)$$

where the higher order terms are normally neglected because the value of θ is in most cases smaller than 0.1 and

$$\theta = \frac{2.303PA}{k\lambda}\left(-\frac{\partial n}{\partial T}\right) \quad (8)$$

A general model for a dual-beam, mode-mismatched thermal lens was subsequently derived by introducing the ratio of pump and probe beam radii inside the sample ($m = (a_p/a_e)^2$) and the parameter describing the position of the sample with respect to the probe beam waist ($V = z_1/z_c$).[16] For steady-state conditions ($t >> t_c$) and small absorbances ($A < 0.1$), the thermal lens signal for a dual-beam experiment can be expressed as

$$S(t) = -2\frac{2.303PAz_1}{\pi ka^2}\left(\frac{\partial n}{\partial T}\right)\tan^{-1}\left(\frac{2mV}{1+2m+V^2}\right) \quad (9)$$

For equal pump and probe beam sizes inside the sample ($m = 1$) and for sample positioned at $z_1 = z_c\sqrt{3}$ (i.e. $V = \sqrt{3}$), the general model gives the same result as the expression for Equation (6) when $t = \infty$ (steady-state thermal lens).

Under particular conditions, such as those encountered when the absorbing species transforms rapidly during the excitation due to photodegradation or other chemical reactions, the changes in absorbance must be considered in the source term. This leads to different time dependencies of the thermal lens signal, depending on the order of the chemical reaction involved.[17,18]

However, it should be noted that it has been recently demonstrated that the thermal lens can also be generated by non-Gaussian excitation sources such as from top-hat beams of incoherent light sources.[19] This is particularly important for the design of practical TLS instruments as application of incoherent light sources would greatly reduce the cost and size of a general TL instrument. Furthermore, the use of a white-light source as the excitation source is potentially advantageous for the development of a practical TL spectrometer with a wide spectral range.

3 INSTRUMENTATION

Despite extensive research directed toward the development of new thermal lens instrumentation, the availability of commercial thermal lens instruments is, at present, limited to only the so-called thermal lens microscopes.[9] Unfortunately, the thermal lens microscope still has relatively limited applicability for general chemical analysis. Thermal lens instruments are, therefore, usually custom-built in laboratories to suit needs of a particular research/measurements. As a result, a substantial number of diverse thermal lens instruments has been reported in the literature. However, according to the principle of their operation, these instruments can, in general, be classified into two basic categories, i.e. single-beam and dual-beam (pump/probe) instruments. It is useful to highlight the basic operational principles of each category in order to understand the operation of some advanced instruments with specific features, which is discussed separately.

3.1 Single-beam Instruments

Single-beam thermal lens spectrometers are unique among thermal lens instruments as the same laser beam is used to both excite the sample and simultaneously probe the thermal lens signal. Single-beam instruments were widely used in the initial stages of thermal lens development. Such systems were primarily used to study the dependence of the thermal lens effect on parameters such as laser power, beam divergence, sample length, concentration, convection, and flow. Application of the technique to chemical analysis did not start until the first report on its use for detection of parts-per-million levels of Cu^{II} as the EDTA complex.[20] In that application, the authors used a single-beam configuration, despite the availability of dual-beam instruments, which should provide better sensitivity. The reason for this and for the relatively frequent use of single-beam instruments, in general, is primarily the simplicity of their construction and ease of operation as compared to dual-beam instruments, namely, only one laser is used to generate and detect the thermal lens.

In a single-beam thermal lens instrument, the laser beam is focused with a lens and modulated by a chopper

or a shutter. After passing the sample, the beam center intensity is usually measured in the far field with a photodiode placed behind a pinhole. The photodiode output is amplified and fed into a storage oscilloscope, which facilitates a recording of transient changes in the beam center intensity.

In principle, any laser operating in the CW mode can be used in a single-beam instrument, provided its power is sufficient to obtain the required sensitivity, and that the wavelength of laser radiation coincides with the absorption band of the compound to be detected. For this reason, single-beam instruments utilizing Ar lasers, which provide discretely tuneable wavelengths over a relatively wide range (several lines from UV to visible region), and powers up to several hundred milliwatts, have been most frequently cited in the literature. However, for excitation at wavelengths not accessible by Ar laser, other lasers, such as He–Cd lasers (441.6 nm), He–Ne lasers (632.8 nm or 3.3 μm), Kr lasers (476.2–799.3 nm), semiconductor lasers (near-infrared), and continuously tunable dye and solid-state lasers, have also been employed in single-beam thermal lens instruments.[21–24]

Several devices such as mechanical choppers, electronic shutters, and, recently, acousto-optic (AO) modulators were used for efficient and accurate modulation of CW laser beams. Most single-beam instruments incorporate an electronic shutter to modulate the laser beam as the shutter can provide relatively long opening periods (up to 1 s) and low repetition rates; these conditions are usually required to record transient thermal lens signals. Mechanical choppers operating at low frequencies (<2 Hz) can also serve the same purpose. Less frequently, higher modulation frequencies, i.e. 10–500 Hz obtained by mechanical choppers or even 150 kHz obtained by AO crystals were applied in single-beam thermal lens measurements. Such modulation schemes are associated with thermal lens detection in chromatography.[7]

As mentioned earlier, the thermal lens strength is most frequently measured as a relative change in the beam center intensity. Only two values (initial intensity $I(0)$ and intensity at some later time during the excitation $I(t)$) of the beam center intensity are in principle needed to calculate the thermal lens strength. Therefore, dual-channel box-car measurement provides a simple, low-cost means to obtain the thermal lens signal. Such detection scheme is, however, hindered by relatively short dynamic range, which can be improved significantly by the so-called kinetic measurement of the thermal lens effect.[21] In such a case, the time-dependent change in the beam center intensity is measured as a transient by a digital oscilloscope and analyzed by nonlinear regression, which averages the short-term noise. In addition to the expanded dynamic range, the kinetic approach also improves the detection limits and allows detection of absorbances as low as 7×10^{-8} with 180-mW laser power.[21] The main drawback of the kinetic thermal lens measurement is the time-consuming averaging procedure, which frequently requires recording of up to 100 transients to minimize the effects of laser noise.

A very efficient and rapid approach to the elimination of signal noise is the lock-in detection. Because lock-in detection is more suited for the dual-beam thermal lens configuration, only a few reports on lock-in detection in single-beam TLS measurements can be found in the literature. Pang and Morris were the first to use lock-in detection in a single-beam instrument.[22] They demonstrated that, by representing the time-dependent thermal lens as a Fourier series, the thermal lens response contains a component at $2f$. Therefore, the application of a lock-in amplifier in its second harmonic mode, to monitor the thermal lens response at twice the modulation frequency, provides a direct measurement of thermal lens signal.

Lock-in detection in a single-beam TLS instrument is also possible by splitting the laser beam into a nonperturbed reference beam bypassing the sample and into excitation beam, which is perturbed by the thermal lens inside the sample[23] or by the application of AO beam modulation.[24] In such a setup, only the zero-order beam from the AO modulator excites the sample, while the first-order component bypasses the sample cell and serves as a reference beam. Another configuration of a single-beam instrument that utilizes lock-in detection was proposed by Erskine and coworkers who used two AO modulators to temporally separate the pump and probe events provided by the same laser beam.[25]

While the single-beam thermal lens spectrometry was proven to be a very sensitive and relatively simple analytical technique, there are certain disadvantages of the single-beam technique, which necessitated further development of thermal lens instrumentation. It is quite obvious that the potentials of the thermal lens technique cannot be entirely exploited in a single-beam measurement. This is because the laser power density, to which the signal is directly proportional, is lower at the optimal sample position than at the focal point. In addition, measurements at different wavelengths are inconvenient or difficult to perform and Equations (5) and (6) suggest a decrease in sensitivity when a long-wavelength laser is required for excitation. Furthermore, most single-beam instruments rely on a time-consuming transient signal recording.

3.2 Dual-beam Instruments

In a dual-beam instrument, the generation and the detection of the thermal lens are achieved separately by a modulated pump beam and a nonmodulated probe beam

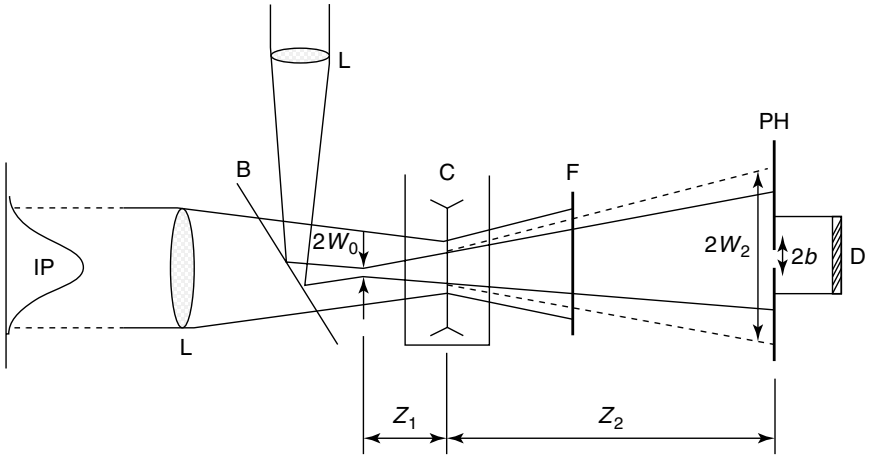

Figure 1 Scheme of the geometric position of laser beams in a mode-mismatched dual-beam thermal lens experiment. IP: intensity profile of the pump beam; L: lenses; B: dichroic mirror; C: sample cell; F: optical filter; PH: pinhole; D: photodiode; w_0: radius of probe beam in its waist; w_2: radius of defocused probe beam at the pinhole position; Z_1: distance between the focal point of the probe beam and the sample cell; Z_2: distance between the sample and the pinhole; b: radius of the pinhole.

respectively (Figure 1). A high-power CW or a pulsed laser usually serves as the source of the pump beam, while the probe beam is derived from a relatively weaker CW laser. By using separate lenses to focus the excitation beam directly into the sample and to mismatch the beam waists of the pump and probe beams, the highest possible thermal lens strength can be achieved. The generated thermal lens produces fluctuations in the intensity of the probe beam that can be sensitively monitored by signal-averaging devices, such as lock-in amplifiers and boxcars, provided that pump beam is filtered out before the detector.

Besides the collinear configuration, the so-called transverse thermal lens configuration is also possible with a dual-beam instrument. In a transverse thermal lens experiment, the excitation beam is focused into the sample perpendicularly to the probe beam (crossed-beam configuration). The monitored volume is, therefore, defined by the intersection of the two laser beams and is usually on the order of a few picoliters. This alignment is particularly useful for small-volume samples and for detection in liquid chromatography and capillary electrophoresis. In a transverse configuration, the signal is not dependent on the sample length but the technique produces good detection limits in terms of absorbance per unit length. Conversely, the collinear configuration provides better absolute sensitivity because of the longer interaction length of the two beams.

In addition to the two most general configurations discussed above, other pump/probe configurations are also possible. For example, pump beam as well as probe beam can both be derived from the same laser. This can be achieved by using a polarizing beam splitter, which partly transmits randomly polarized laser light. Such a compact single-laser, dual-beam apparatus was developed further and adopted for liquid chromatographic detection.[7]

A particular configuration that exploits a single beam for a pump–probe TLS experiment is the so-called rotoreflected laser beam thermal lens, which exploits the change in the polarization of laser beam when reflected from a mirror.[26] With the reflecting mirror positioned at $(z_c\sqrt{3})/2$ from the sample cell, the retroreflected beam probes the thermal lens generated at its focus and at the same time generates another thermal lens, which is probed by the same beam like in a usual single-beam configuration. This results in an almost threefold increase in the concentration sensitivity and in about 12-fold increase in the absolute sensitivity. Larger enhancement in absolute sensitivity stems from the fact that the thermal lens effect in a rotoreflected instrument originates from a volume defined by the beam waist, which is four times smaller than in the case of a conventional single-beam instrument.[26]

Thermal lens instruments with oppositely propagating pump and probe laser beams were also described. Among them an interesting instrumental design was reported by Higashi and coworkers,[27] who used a prism to ensure good overlapping of oppositely propagated pump and probe beams. Such prisms can also replace filters in instruments where pump and probe beams propagate in the same direction.

Different from single-beam instruments, pulsed lasers can be used in dual-beam thermal lens instruments. As a consequence, a variety of lasers can be used for excitation in dual-beam TLS instruments, ranging from CW gas lasers (He–Ne, He–Cd, Ar, Kr, CO, and CO_2), dye and semiconductor lasers, to pulsed dye, N_2, CO_2, and Nd:YAG lasers. Continuously tunable

thermal lens spectra can be obtained by using a tunable IR laser generated by a stimulated Raman effect, as already reviewed.[7] Recently, spectrally tunable Ti-sapphire and F-center lasers,[28,29] as well as Er-doped fiber amplifiers,[30] were also used as excitation in TLS.

Laser power is not important for the selection of the probe beam source in a dual-beam instrument. Attention must be paid to laser stability instead. It is therefore not surprising that, almost exclusively, low-power He–Ne lasers, which are known for their stability and reliability, were used to probe the thermal lens effect in instruments with a dual-beam configuration. Only few exemptions can be found in the literature, which rely on application of He–Cd lasers or Ar laser.[7]

It is interesting to note that, in the early applications of dual-beam thermal lens spectrometry, which were less concerned with the optimization of technique's sensitivity, unfocused pump and probe laser beams were used. In mode-matched applications, both beams were focused by a single lens or concave reflector. Despite strongly aberrant thermal lens generated in experiments exploiting focused pump beams and nonfocused probe beams, good detection limits were obtained. Similarly, significant improvements of sensitivity were achieved in the mode-mismatched dual-beam configuration, where the sample is put at the waist of the pump beam where the power density of excitation light is the highest.[7]

3.3 Differential Thermal Lens Instruments

The dependency of the thermal lens on the beam's position offers another interesting feature of TLS technique. This is the capability of differential absorption measurements, which stems from the fact that signals of the same absolute magnitude, but opposite in sign, are produced when the same sample is placed at two positions symmetrically with respect to the probe beam waist. As the effects of thermal lenses on the laser beam are additive, no thermal lens effect is observed at the detector when two identical samples are positioned symmetrically with respect to the probe beam waist. This implies the possibility of automatic blank signal elimination and improved limits of detection.

The concept of differential thermal lens spectrometry was introduced by Dovichi and Harris,[31] who constructed the first differential single-beam thermal lens instrument. As a result of up to 99% efficiency in background signal subtraction, which can be achieved by the differential configuration, a limit of detection equal to $A = 6.3 \times 10^{-7}$ was achieved.

Differential single-beam thermal lens configuration was also successfully applied to compensate for solvent absorption as well as for eluent flow oscillations in chromatographic detection.[32]

Further progress in differential thermal lens spectrometry was made with the introduction of differential dual-beam instruments with collinear geometry of pump and probe beams.[33] Despite the fact that it requires relatively more laborious alignment procedure compared to single-beam differential instruments, it was demonstrated that 95–98% of the solvent's thermal lens effect can be compensated. It should, however, be noted that, different from the conventional dual-beam thermal lens instruments, in a differential configuration the pump beam is not focused inside one of the sample cells, but approximately at the same point as the probe beam, i.e. in between the two sample cells to ensure the same power density in both cells.

To ensure the optimal differential response of single – as well as dual-beam differential thermal lens instruments, power losses due to reflections and absorption of light in the first cell must be taken into account. Compensation for higher power at the first cell, which consequently produces a higher thermal lens signal, is usually obtained by slightly displacing the first cell from its calculated optimal position, until a zero signal is observed during the alignment procedure with two identical samples (solvents). However, in the presence of large background absorption, like in the case of indirect photometry, such compensation is not practical and might lead to substantial loss of sensitivity.

For differential thermal lens measurements under high background conditions, the so-called obliquely crossed differential thermal lens spectrometer was proposed for indirect detection of fatty acids after HPLC separation.[34] Instead of a collinear configuration, an oblique overlapping of probe and excitation beams, which can be obtained by splitting the pump laser beam into two beams of equal intensity, was used. The two excitation beams spatially overlap with the probe beam under a small angle (about 2) to ensure the maximal effect of the generated thermal lens on the probe beam. Different from the traditional pump/probe configuration, the two excitation beams are not modulated, and therefore they produce a steady-state thermal lens in each of the sample cells. Lock-in detection is possible by modulating the probe beam, which detects only changes in the differential thermal lens signal and not its real magnitude. This is, however, sufficient to observe small differences in absorbance (LOD $= 2 \times 10^{-7}$) inside two flow cells, resulting from dilution of highly absorbing eluent by nonabsorbing analytes, which manifested as chromatographic peaks.

A similar approach was also applied for differential TLS measurements in the mid-IR spectral region (Figure 2), where the background absorption by solvents is usually very high.[35] The angle of overlapping of pump and probe beams is less critical in such a case because the detection in

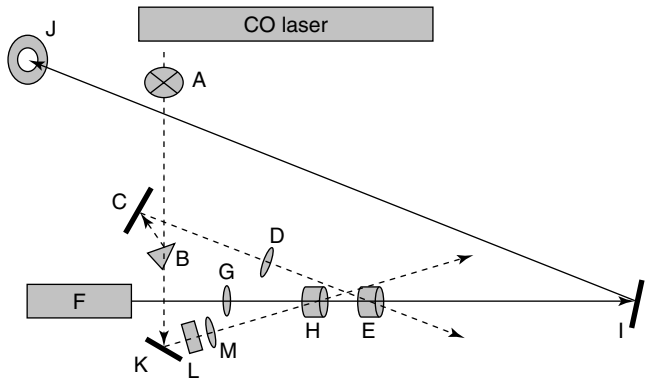

Figure 2 Block diagram of a differential thermal lens spectrometer for measurements in the infrared. A: mechanical chopper; B: wedge beamsplitter; C, K, I: mirrors; D, M: ZnSe lenses; G: glass lens; E, H: flow-through cells; F: He–Ne laser; J: photodiode; L: variable beam attenuator.

mid-IR requires short optical path lengths (100–200 μm). For excitation in the spectral range of the CO laser, used for detection of carboxylic acids, efficient elimination of background absorption was demonstrated even for high backgrounds such as those encountered in the case of aqueous solutions.

3.4 Multiwavelength and Tunable Thermal Lens Spectrometers

In addition to the quest for higher sensitivity, the development of dual-beam instruments was prompted by the need for multiwavelength capability of TLS measurements. Several tunable thermal lens spectrometers appeared among the first dual-beam thermal lens spectrometers. They are characterized by their ability to measure thermal lens signals over a certain range of wavelengths. With regard to their design and operation, they are very similar to conventional dual-beam thermal lens instruments. The most significant difference is the use of continuously or line tunable lasers for excitation of the sample instead of a laser operating at a discrete wavelength.[7] Tunable thermal lens spectrometers were most frequently used to obtain absorption spectra of weekly absorbing samples or spectra resulting from overtone vibrational transitions and multiphoton absorptions. More recent applications include measurements of TLS spectra of lanthanide ions in aqueous solutions, which also demonstrated that the enhancement of TLS signal is possible in cases where sample matrix absorbs the probe beam wavelength.[28] In general, however, the performance of thermal lens scanning spectrometers is hindered by the relatively time-consuming measurements over a wide range of wavelengths. This is an important factor in different analytical procedures such as chromatography and electrophoresis, where the continuously changing composition of flowing sample emerging at the detector demands real-time measurements, i.e. measurement of the thermal lens signals at several wavelengths within a few seconds. Besides, simultaneous measurements at two or more wavelengths, which provide useful information concerning the composition of the analyte, cannot be performed by usual tenable thermal lens instruments. These were the main reasons that prompted the development of the so-called multiwavelength – dual-beam or ''multicolor'' – instruments.

The first dual-wavelength thermal lens instrument was developed by deriving two excitation beams of different wavelengths from the same argon ion laser operating in a multiline mode and by separating the emission lines by means of an Amici prism.[36] Both beams were modulated by the same mechanical chopper and were aligned collinearly by a mirror and a beam splitter. As a result, the sample was alternately excited by two beams of different wavelengths modulated at the same frequency but 90 out of phase to each other. A dark period followed each excitation in order to allow the sample to return to its original thermal state. The magnitudes of thermal lens signals were obtained from a digital scope. The sensitivity of this instrument was shown to be comparable to sensitivities of single-wavelength instruments. In addition, it was demonstrated that different compounds in liquid and gaseous samples can be identified by measuring the ratios of thermal lens signals at different wavelengths. Furthermore, the instrument enables elimination of the annoying and wavelength-independent background absorption by measuring and subtracting thermal lens signals at two wavelengths (provided the species of interest absorbs only at one wavelength). This implies the possibility for real-time automatic background correction, which can be performed from a single measurement even in the presence of highly absorbing interfering species.

Dual-wavelength thermal lens spectrometers have undergone further development by the construction of an instrument with a crossed-beam configuration for measurements in small-volume samples. An argon ion and a He–Ne laser, both operating in a single line mode, were used for excitation, and the probe beam was derived from a 1% reflection of the He–Ne laser beam at the beam splitter, like in the case of single-laser, dual-beam instruments.[37]

A different ''two-color'' thermal lens instrument was developed by Earle and Dovichi, who used a crossed-beam configuration for detection in capillary zone electrophoresis.[38] In this instrument, the two laser beams from a He–Ne and a He–Cd laser are modulated by two mechanical choppers operating at different frequencies. The modulated beams serve to excite the sample and, at the same time, to probe the thermal lens generated by the

second beam of different wavelength. The thermal lens signals are demodulated by means of two photodiodes connected to adjacent lock-in amplifiers. The optical system is identical (with the exception of an additional chopper, mirror, and photodiode) to that employed in conventional crossed-beam thermal lens instruments. This facilitates the alignment and makes the operation of dual-wavelength thermal lens instruments by less skilful personnel possible.

Xu and Tran[39] demonstrated that even collinear alignment of four excitation beams and one probe beam can be realized accurately. They took advantage of the multiwavelength emission from the argon ion laser and utilized two additional wavelengths, which were not exploited in the first dual-wavelength instrument. By introducing two additional beam splitters and by replacing the chopper with four synchronized electronic shutters, they constructed the first multiwavelength thermal lens spectrometer operating at four different wavelengths. After initial alignment difficulty, handling of the instrument is easier because of its good stability, which stems from the fact that all the beams are derived from the same laser.

This group of instruments has a potential to simultaneously determine concentrations of two or more compounds in a mixture, which is directly associated with the substantially improved selectivity of dual- and multiwavelength instruments compared to single-wavelength instruments. However, each additional laser beam or optical component makes their alignment and operation increasingly complicated. To overcome such difficulties, an acousto-optic tenable filter (AOTF) was incorporated into the previously described dual-wavelength or four-wavelength instrument in order to develop a fast scanning multiwavelength thermal lens spectrophotometer with a wide tuning range (457.9–514.5 nm).[40] Owing to the properties of AOTF, which enabled high-speed sequential wavelength access, there was no need for a mechanical chopper or electronic shutter. Furthermore, several optical components (mirrors, beam splitters, prism) could be omitted, which made the alignment procedure simpler and comparable to single-wavelength pump/probe instruments. By appropriate selection of radiofrequency applied to the AOTF, all six wavelengths emitted by the Ar ion laser operating in a multiline mode (457.9, 476.5, 488, 496.5, 501.7, and 514.5 nm) were exploited to excite the sample during a time period of 1.5 s. Through its multiwavelength capability, the described thermal lens spectrophotometer, whose limit of detection is comparable to other dual-beam thermal lens instruments, provides fingerprints of analytes and can be used to analyze samples of up to six different components. In principle, a truly multiwavelength thermal lens spectrophotometer for real-time measurements can be constructed using a combination of lasers and an acousto-optic tunable filter.

3.5 Circular Dichroism TLS Instruments

Originating from dual-wavelength instruments, TLS instruments were developed for measurement of circular dichroism (CD) of optically active samples. TL-CD instruments are of particular importance as they enabled, for the first time, CD measurements of weakly absorbing chiral samples in volumes of few microliters. In such an instrument, the sample is sequentially excited by left circularly polarized laser light (LCPL) and right circularly polarized laser light (RCPL). The difference between the thermal lens signal generated by LCPL and RCPL in a transverse pump/probe geometry corresponds to a TL-CD signal. The sensitivity of this instrument is higher compared to that of conventional CD spectropolarimeters, and provides detection limits of 180 ng for (−)-tris(ethylenediamine)cobalt(III) in an 8-μL optically active sample.[41] A similar instrument based on a collinear configuration was subsequently developed to further increase the sensitivity of the instrument. In an equal volume, this instrument is capable of detecting as low as 5 ng of the aforementioned Co complex.[42] The instrument still cannot measure the CD signal directly. For this reason, the third generation of TL-CD instruments was developed. In such an instrument, the LCPL and RCPL are generated by the means of a Pockels cell that enables consecutive excitation by the LCPL and RCPL at low frequency (2 Hz) without any dark period between the two excitations. The difference in the LCPL and RCPL thermal lens signals, i.e. the TL−CD signal, can therefore be obtained in real time by simply using a lock-in amplifier. By using such an instrument, a direct and real-time determination of the chirality and optical purity of an effluent eluted from a liquid chromatograph was demonstrated for the first time.[43] A detection limit of 7.2 ng was achieved by this chiral detector for (−)-tris(ethylenediamine)cobalt(III), and for the corresponding (+) enantiomer, when these two enantiomers were chromatographically separated from the corresponding racemic mixture.

3.6 Miniaturization of Thermal Lens Instruments

Thermal lens instruments that have been so far described in the literature are, with almost no exemption, based on the far field detection of the thermal lens signal. Such experimental configuration frequently necessitates optical paths of several meters to fulfill the far field limit requirements. This makes thermal lens instruments relatively large and unwieldy compared to commercially

available conventional spectrophotometers. Another disadvantage of TLS instruments is their difficult alignment, and the influence of laser pointing and mode instability. All these effects can be minimized by a smaller and compact configuration of a thermal lens instrument, which could be designed on the basis of the near field detection as proposed by Long and Bialkowski.[44]

In fact, the analysis of positional dependence of thermal lens effect reveals that a near field maximum of thermal lens signal can be predicted, if simplifications leading to the far field approximation are not used in the derivation of thermal lens theory. For a near field thermal lens detection, the sample should be placed into the converging part of the focused probe beam, while the detector should be located at the probe beam focal point. Although the sensitivity of the thermal lens technique is slightly reduced in the case of near field detection, this detection scheme should offer several advantages, which include minimized aberration effects due to reduced probe beam spot size, and much more compact construction of the instrument as optical paths of centimeters are needed compared to meters required in far field detection. The difficulty that limits the absolute exploitation of the near field detection is the fact that the beam size should be larger than the limiting aperture at the detector.

Another problem that is frequently encountered with the application of large laser systems is the difficulty of delivering the laser light to a remote location. In addition to compact flexible lasers, optical fibers provide a solution in such cases. It is interesting that optical fibers were quite frequently applied in thermal lens spectrometry as limiting apertures for probe beam center monitoring and to deliver the probe beam light to the photodetector.[7]

Less frequently, optical fibers were used in thermal lens spectrometers to deliver the excitation light to the sample. Bialkowski demonstrated that the mode and pointing variations in the laser can be reduced when the excitation light is delivered through a silica optical fiber.[45] On the other hand, Imasaka and coworkers used a couple of optical fibers in a single-beam instrument to deliver the excitation light directly into the sample and to probe the signal intensity.[46]

The most detailed theoretical and experimental investigation on the applicability of optical fibers in thermal lens spectrometry was, however, given by Rojas and coworkers,[47] who constructed a dual-beam optical-fiber thermal lens spectrometer. By considering the finite nature of the optical fiber as the limiting aperture for probe beam sampling, they have demonstrated that it is not necessary to place the optical aperture at long distances from the sample to obtain the maximum signal if the aperture is sufficiently small. Another interesting application of optical fibers is the use of Erbium-doped optical fiber amplifier, where the fiber itself serves as the light source.[30]

Besides the near field detection of thermal lens signal, the size of thermal lens instruments can be substantially reduced by application of small lasers such as diode lasers, which are more frequently used as probe beam sources in thermal lens spectrometry. An inexpensive, small-size tunable dual-beam optical fiber thermal lens spectrometer was developed by using a temperature-controlled GaAlAs diode laser.[48] In this work, all the possibilities for miniaturization of thermal lens instruments mentioned in this section were exploited.

As already mentioned, conventional light sources offer additional possibilities in miniaturization of TLS instruments, as shown in the case of top-hat[19] excitation beams as well as for the application of specially designed sample cells or in a microchannel, which assist in generating a temperature gradient inside the sample.[49,50]

4 UNIQUE PROPERTIES AND CAPABILITIES OF THERMAL LENS TECHNIQUES

4.1 High Sensitivity: Trace Chemical Characterization

4.1.1 Environmental Applications of Thermal Lens Techniques

Several applications of TLS for analysis of environmental samples and studies of relevant environmental processes have been reported and reviewed in papers and books recently.[51,52] However, no detailed validations were carried out of the proposed new analytical methods. The first reported validation of TLS was performed for batch mode determination of Cr^{VI} using a standard reference material and was followed by comparative determination of chromium species (Cr^{III} and Cr^{VI}) in drinking water samples by ion chromatography with spectrometric and TLS detection. Good agreement of measured values with reference values and those provided by an independent technique have definitely established TLS as an accurate and reliable analytical tool.[53]

The sensitivity of TLS determination of Cr^{VI} was further improved by performing the measurements in a flow injection analysis (FIA) mode. It is well known that metal–DPC complexes are photolabile and Cr–DPC was shown to degrade rapidly under the influence of intensive (100–500 mW) and tightly focused laser light. The application of FIA is therefore advantageous as it reduces the exposure of the analyte to laser light, thereby reducing photodegradation of Cr–DPC, which is known to hinder the sensitivity. Furthermore, the

uncertainty of the measurement arising from uncontrolled photodegradation in batch mode measurement is also reduced. As a result of measurements in the FIA mode, the LOD for TLS determination of Cr^{VI} was reduced down to 67 ng L^{-1},[54] despite some loss of sensitivity arising from the effects of the flow, and with the absence of added organic solvents to improve thermo-optical properties. This represents an improvement by almost a factor of 2 compared to the batch mode measurement.[53]

TLS determination of various inorganic species (heavy metals, inorganic anions) is, however, hindered by lower enhancement factors and associated lower sensitivity of water-soluble analytes, which is also unavoidable in combination with ion chromatography or capillary electrophoresis. The second limitation is the availability of excitation sources, appropriate for the detection of ionic species, which show weak absorbances of visible or UV light. Pre- or postcolumn derivatization must therefore be applied to convert the analytes into compounds with higher extinction coefficients and/or to shift their absorption maxima into the visible spectral range, as was proven to be effective in the case of IC-TLS, where coloring reagents and ligands such as 1,10-phenanthroline,[55] pyridine-2,6-dicarboxylic acid (PDCA),[56,57] 1,5-diphenylcarbazide (DPC),[54,56,57] and 4-(2-pyridylazo) resorcinol (PAR)[58] were used for derivatization of various heavy metals and their species.[8]

As TLS is a background-limited method, the selection of appropriate derivatization reagent is of particular importance not only from the point of selectivity and sensitivity (high extinction coefficients) but also to assure the low LODs. As demonstrated for the determination of Fe^{III} and Fe^{II} ions by IC-TLS,[55] colorless reagents, e.g. 1,10-phenanthroline, are advantageous and provide lower LODs compared to reagents with relatively high background absorbance, such as PAR. For the given case, two and four times lower LODs were obtained for IC-TLS determination of Fe^{III} and Fe^{II}, respectively, when 1,10-phenanthroline was applied for postcolumn derivatization instead of PAR. The lowest LODs achieved for Fe^{II} by IC-TLS (25 and 5 $\mu g\,L^{-1}$, respectively) represent a sevenfold improvement compared to UV–vis spectrometry and 15-fold improvement compared to amperometric detection.

Similar improvements in LODs, compared to ion chromatography relying on UV–vis detection, were also reported for the IC-TLS determination of Cr^{VI} and Cr^{III}, where both species are separated as anions after precolumn derivatization of Cr^{III} with PDCA. For detection of Cr^{VI}, a postcolumn derivatization with DPC is needed.[56,57] Comparative analysis of drinking water samples has revealed another advantage of TLS detection, which was found to be much less affected by light scattering, resulting from CO_2 released in acidified samples containing higher levels of carbonate. As a result of light scattering, UV–vis detection was subject to up to 20% positive errors.[8]

By exploiting derivatization as well as addition of organic solvents such as methanol, acetone, or acetonitrile, it was possible to significantly improve the sensitivity of the IC-TLS. Addition of acetonitrile to the eluent and postcolumn reagent (30% v/v) enables simultaneous determination of Cr^{VI} at the 0.1 $\mu g\,L^{-1}$ and of Cr^{III} at the 10 $\mu g\,L^{-1}$ level.[57] The improvement stems from the fact that, due to lower k and higher $\partial n/\partial T$ of acetonitrile compared to water, the enhancement factor was increased by a factor of 5.4 compared to measurements in an aqueous eluent (details on enhancement due to k and $\partial n/\partial T$ are discussed in detail in Section 4.4). Such a low LOD value for Cr^{VI} is comparable to the LOD for ET-AAS, which is however not capable of performing on-line detection in a separation of both Cr species.

Applications of TLS for determinations of compounds such as pesticides and pharmaceuticals by using capillary electrophoresis (CE) as a separation technique were reported.[59] Examples of CE-TLS include detection of chloramphenicol, diclofenac, pentoxifyllin, and oxprenolol, which belong to the group of pharmaceuticals that were recently recognized as emerging pollutants of aquatic environment. The reported limits of detection for individual drugs were in the range of 4.5×10^{-5} M.[59]

Other applications of TLS for the detection of environmental pollutants include the determination of pesticides in water samples, which were developed by simply adopting previously developed methods for analysis of foodstuff.[60,61] This includes monitoring of toxicity during the photodegradation of organophosphate pesticides and related photocatalytic processes as well as in investigations of advanced oxidation methods for treatment of waters contaminated by OP pesticides.[62] Fast response of FIA-TLS and little sample handling enable quasi on-line monitoring (3–5 min time resolution) of degradation processes, which in general lasts for 1–2 h. Inhibition of AChE activity, which correlated well with the concentrations (below 1 ppm) of inhibiting compounds detected by GC-MS, reveals the formation of toxic degradation products, which cannot be detected by monitoring the disappearance of the parent compound to determine the end point of degradation process.[63,64] Because of the much faster response and high sensitivity for detection of the TLS method based on AChE inhibiting compounds, the method was clearly found advantageous compared to toxicity testing based on the inhibition of fluorescence from *Vibrio fischeri*,

which is most frequently applied in processes for removal of OPs, but is three times less sensitive for the detection of oxo-organophosphates compared to phosphorothionates.[62]

Important progress in TLS applications for environmental research has also been made by the development and application of a novel double dual-beam TLS instrument designed for on-line studies of phytoplankton cell lysis, which was based on nonselective detection of an entire group of pigments (mainly carotenoids and chlorophylls) released from phytoplankton cells after the damage or decay of the cell membrane. A dedicated double dual-beam TLS spectrometer enabled on-line monitoring of phytoplankton cell culture media pumped continuously from a control sample and from a sample exposed to effects causing the cell lysis (salinity shocks, cytotoxins).[65] The increase in absorbance, due to the contributions of individual pigments from lysed phytoplankton cells, was promptly detected in the flowing cell culture media by TLS, and the signal reached a steady value when the lysis was complete. Owing to insufficient sensitivity, spectrophotometry failed to indicate any change in absorbance under the same experimental conditions even in the case of complete lysis. Without any need for sample pretreatment or preconcentration, the TLS method enables the detection of 6×10^6 lysed cells per liter, which is in the range of cell densities found in the natural sea waters. TLS can thus be utilized in monitoring and investigating the early stages of algal blooms, which are not well understood yet.

Identification of plankton species participating in various stages of algal blooms is also very important for proper understanding of these natural phenomena and of environmental conditions that trigger them. Chemotaxonomy based on determination of pigments characteristic for plankton taxonomic groups can be adopted for such investigations. For example, fucoxanthin and diadinoxanthin as fingerprint carotenoids for diatoms can be efficiently determined by HPLC-DAD and used to confirm the presence of diatoms. However, the two pigments cannot be used to discriminate between species of diatoms such as *Phaeodactilum tricornutum* and *Skeletonema costatum.* This is because HPLC-DAD cromatograms of both species are actually identical with only two carotenoids (fucoxanthin, diadinoxanthin) detected. On the contrary, HPLC-TLS, owing to higher sensitivity, was demonstrated to be capable of detecting over 20 additional nonidentified pigments (presumably carotenoids) present in minor concentrations, and therefore not detected by HPLC-DAD.[66] High selectivity and sensitivity are required to distinguish among pigments from many of possibly present species, without preconcentration and additional sample treatment (filtration of large volumes of sea water), which might cause additional cell lysis and therefore affect the results. Therefore, a novel HPLC-TLS method for the detection of phytoplankton pigments (carotenoids and chlorophylls) in isocratic elution mode was developed for such tasks. Up to 27 pigments from the groups of carotenoids and chlorophylls were successfully separated and detected in a mixed standard solution and in extracts of phytoplankton cultures by the applied HPLC-TLS protocol, which required 45 min for completion of a chromatographic run.

For similar reasons, the HPLC-TLS has been applied for studies of xanthophyll cycles in marine phytoplankton. In xanthophyll cycles, the light-harvesting pigments are transformed into photoprotecting pigments under the influence of light. Such a transformation of diadinoxanthin into diatoxanthin was clearly observed by HPLC-TLS (LOD = 0.036 and 0.028 $\mu g\,L^{-1}$, respectively) in samples of laboratory-grown *Amphidinium carterae, Emiliania huxleyi, Skeletonema costatum,* and *Phaeodactylum tricornutum*, exposed to artificial daily light cycle. Furthermore, changes in concentrations of minor pigments, which could not be detected by HPLC-DAD, were observed in *Chroomonas salina* grown under similar conditions. This was the first experimental indication for the existence of a xanthophyll cycle in this species.[66]

4.1.2 *Applications of Thermal Lens Techniques in Agriculture and Food Sciences*

The quality and safety of food has become a subject of high priority in recent years. Development of new TLS methods that can determine (i) compounds with adverse health effects (pesticides, fatty acids) present in agricultural products and foodstuff; (ii) compounds that are beneficial (e.g. antioxidants such as carotenoids); and (iii) markers of food quality and adulteration has been a subject of intense study in recent years. Most applications in this field rely on the use of TLS as the detection method in liquid chromatography or flow injection analysis. However, a few applications in batch mode are also reported.

Free fatty acids (FFAs) in liquid samples were determined by TLS measurements in the mid-IR region. By measuring the concentration of stearic acid in CCl_4 based on a vibrational band of a fatty acid dimer with the 934.9 cm^{-1} emission line of a CW CO_2 laser, it was possible to determine FFAs at concentration levels below 1%. By exploiting excitation at 965 cm^{-1} on the same IR TLS instrument, detection of 0.002% trans fatty acids (*trans*-hexadecenoic and *trans*-octadecenoic acids) in margarine was reported.[52,67]

Batch mode TLS detection in the visible spectral range was utilized for the determination of tanines in wines.[68]

The high sensitivity of TLS detection makes it possible to achieve a LOD of 5 ng mL^{-1} for folic acid even with 25 000-fold dilution of original samples. Highly sensitive HPLC-TLS detection of carotenoids was exploited for the determination of carotenoids and quality control of fish body oils, fish-oil-based drug supplements, as well as olive and other vegetable oils.[8,69–72] The method relies on matrix-matched calibration, which is facilitated by the fact that no time-consuming extraction of carotenoids from the sample matrix is required. Instead, a simple 100- to 400-fold dilution of samples in a 50 : 50 v/v mixture of eluent (9 : 1 methanol : THF) and chloroform prior to injecting of diluted samples into the chromatographic column (10-μL injection loop). Satisfactory separation of different carotenoids, particularly of α-carotene, β-carotene, lycopene, and their isomers, is achieved with a 12–15 min[70] isocratic chromatographic run, providing LODs similar to those reported for extracted samples. This represents more than three times higher sample throughput compared to HPLC-DAD methods for carotenoids determination in similar samples, not taking into account much faster sample preparation step in case of HPLC-TLS. This makes HPLC-TLS suitable as a fast screening method for the evaluation of the quality and eventual adulteration of foodstuff. The latter application was demonstrated in a paper in which TLS was used as the detection technique in HPLC for analysis of virgin olive oils and other vegetable oils.[71]

Simple dilution of samples cannot be applied for analysis of products such as fruit juices and foodstuff from tomatoes. Nonetheless, the high sensitivity of TLS again facilitates the analysis by requiring five times smaller amounts of samples (2 g or 10 mL in the case of juices) and thus five times less organic solvents and time for extraction procedure. HPLC-TLS was successfully applied for the determination of lycopene and β-carotene in tomato pastes, ketchups, and other tomato products,[73] as well as for the determination of various carotenoid compounds in fruit juices, which can serve as indicators of purity or adulteration of orange juices.[69] Thermal treatment of an orange juice or vegetable oil can also be recognized by the disappearance or decrease of carotenoid compounds and appearance of oxidized xanthophyll compounds, which can be readily distinguished in HPLC-TLS chromatograms at concentrations as low as 0.1–0.5 μg L^{-1}.[69,72]

A simple and sensitive HPLC-TLS method was reported for simultaneous determination of four neonicotinoid insecticides, i.e. thiamethoxam, imidacloprid, acetamiprid, and thiacloprid.[60] The method provides sensitive, selective, and reproducible trace-level determination of these four neonicotinoid insecticides and offers the LODs lower by 2.5–8.5 times for thiamethoxam (LOD = 15 μg L^{-1}), acetamiprid (LOD = 3.2 μg L^{-1}), and thiacloprid (LOD = 7.5 μg L^{-1}) compared to HPLC-DAD with similar RSDs. The LOD value for imidachloprid was equal to the LOD provided by HPLC-DAD. The differences in LODs were attributed to differences in absorption spectra and extinction coefficients of investigated compounds, and to the fact that HPLC-DAD measurements were performed at absorption maxima, while TLS detection was limited to the one available laser excitation wavelength. In the case of acetamiprid and thiacloprid, the absorption maximum overlaps well with the excitation wavelength used for TLS detection (244 nm). For thiametoxam and imidachloprid, the absorption maxima are however at 254 and 270 nm, respectively. The method was successfully tested for the determination of all four insecticides in real samples such as potato and peppers. The HPLC-TLS results agreed well with HPLC-DAD data, showing a maximal 15% discrepancy. In addition to lower LOD, the advantage of HPLC-TLS is evident in terms of smaller sample size and shorter time needed for its preparation.

In the case of fatty acids and fatty acid esters, the lack of suitable excitation sources in the UV–vis spectral range was successfully overcome by the development of HPLC-TLS methods utilizing a CO laser as excitation source, which also enabled recording of TLS spectra of investigated compounds in organic solvents.[8] By performing HPLC analysis of a commercial mixture of C18 fatty acids at 1734 cm^{-1} CO laser emission line, it was demonstrated that the infrared HPLC-TLS method can discriminate fatty acids from higher concentrations of co-eluting noncarboxylic compounds such as longer chain alcohols (octanol, decanol), which still exhibit week absorbance at the excitation wavelength. Such discrimination was not possible in the case of refractive index detectors, which, on the other hand, were not inferior in terms of LODs (0.03 % for oleic acid) as the LODs of HPLC-TLS were very much hindered by the relatively high background absorption of eluents in the IR spectral range.[69,74]

Substantial amount of work has recently been conducted on the utilization of TLS as a detection technique in FIA. FIA-TLS was used efficiently for determination of organophosphate (OP) and carbamate pesticides in fruit juices and vegetables. For this purpose, a dual-beam, mode-mismatched pump/probe TLS spectrometer was coupled to a FIA system with an incorporated bioanalytical column containing acetylcholinesterase (AChE) immobilized on glass bids.[8,61,69]

The method was successfully applied for highly sensitive determination of organophosphates such as paraoxon (LOD = 0.2 μg L^{-1}) and carbamates such as carbofuran (LOD = 1 μg L^{-1}) in samples of tap water and spiked

fruit juices and in samples of vegetables such as onion and lettuce. The FIA-TLS system was calibrated by using paraoxon standard solutions, and the concentrations of pesticides detected in each sample were expressed in terms of paraoxon equivalents. Taking into account the differences in the toxicities of pesticides (LD_{50} values for rats) present in the sample, the determined paraoxon equivalent concentrations were reported to agree well with concentrations of individual pesticides (carbofuran, propamocarb, oxydemeton-methyl, and parathion-ethyl) determined by GC-MS.[61]

4.1.3 *Biochemistry and Biomedical Applications of Thermal Lens Techniques*

High sensitivity and small-volume sample capability characteristic of thermal lens technique makes it particularly suited for measurements of biochemical, medical, and pharmaceutical samples as these samples are often available in small quantity and low concentrations. Response of individual cells to antitumor drug was successfully monitored using the thermal lens technique.[75]

Table 1 Biochemical and biomedical applications of thermal lens techniques

Analyte	References
Micro-ELISA with microchip device and thermal lens microscope	86
Determination of catecholamine on a microchip by thermal lens microscope	87
Assay of spherical surface of blood cell by thermal lens microscope	80
Detection and measurement of a single blood cell surface antigen by thermal lens microscope	82
Analysis of serum proteins adsorbed to hemodialysis membrane by thermal lens microscope	83
Determiation of critical increment of Lewis blood group antigen in serum	84
Sub-attomole molecule detection in a single cell in vivo by flow cytometry with thermal lens detection	81
Determination of drug concentration in a renal tubule of fixed kidney by thermal lens microscope	85
Analysis of a single biological cell in water by thermal lens microscope	79
Single cell analysis and monitoring of cytochrome c distribution during apoptosis process by thermal lens microscope	88
Determination of carcinoembryonic antigen in human sera by integrated bead-bed immunoassay in a microchip with thermal lens microscopic detection for cancer diagnosis	89
Individual cell in blood and lymph flow by the thermal lens technique	76
Response of individual cell to antitumor by the thermal lens technique	75

However, it is often necessary to combine and/or modify conventional thermal lens instrument to further increase its sensitivity and reduce the amount of sample needed. For example, thermal lens was combined with flow cytometry for the determination of individual cells in blood and lymph flow.[76] The most notable development was made by the Sawada group on the thermal lens microscope, which combines advantages of microscope (small-volume sample, high spatial resolution) with the thermal lens technique (high sensitivity).[77,78] In fact, in addition to the small sample size and high sensitivity, the thermal lens microscope can also be used to determine nonfluorescent molecules without receiving serious effects of light scattering in/on various condensed phase substances and it can be applied for imaging of the distribution of nonfluorescent molecules by scanning on the sample. This makes the thermal lens microscope (TLM) suited for ultrasensitive analysis and imaging of biomedical substance in/on a single cell and microfabricated chemical devices (microfluidic devices). For instance, the TLM was successfully used in the analysis of a single biological cell in water,[79] the assay of spherical cell surface molecules,[80] the sub-attomole molecule detection in a single biological cell in vitro,[81] the detection and measurement of a single blood cell surface antigen,[82] the analysis of serum proteins adsorbed to a hemodialysis membrane of hollow fiber type,[83] the determination of critical increment of Lewis blood group antigen in serum by cancer,[84] and the quantitation of drug concentration in a renal tubule of fixed kidney.[85] Synergistically combining TLM with microfluidic devices makes it possible to perform measurements and assays that are otherwise not possible. These include a microchip-based, enzyme-linked immunosorbent assay (micro-ELISA) system with thermal lens detection,[86] the determination of catecholamine on a microchip,[87] single-cell analysis and direct monitoring of cytochrome c distribution during apoptosis process,[88] and the determination of carcinoembryonic antigen in human sera for cancer diagnosis.[89] Specifics of these studies, which are discussed in more detail in Section 4.2.1., are summarized in Table 1.

4.1.4 *Thermal Lens Techniques in the Near- and Middle-Infrared Region*

As described in the previous section, thermal lens measurements are based on the use of laser as the excitation source. Therefore, the spectral range in which measurements can be performed is dependent on the availability of lasers in that region. To date, most of the thermal lens work was in the ultraviolet and visible region as lasers are readily available for this region at reasonable cost. Recently, lasers in the near- and middle-infrared

region, for example, Nd : YAG, Ti-Sapphire, F-center, and diode lasers, have become available at reasonable price and high reliability and are easier to use. As a consequence, thermal lens measurements can now be performed in spectral regions, which hitherto were not possible. For example, by using a Ti-Sapphire laser, which is tunable from ~865 to 1050 nm to excite overtone and combination transitions of O–H and C–H groups, Tran and coworkers were able to determine chemical and isotopic purities in various solvents including water in D_2O and in tetrahydrofuran at levels as low as 0.006 and 0.3% (v/v).[90] They also determined simultaneously water and DMSO-h_6 in DMSO-d_6 and CD_3OH in CD_2HOH and CDH_2OH at levels as low as 10^{-3}%.[91] By replacing the near-infrared Ti-Sapphire laser with an F-center laser, which can spectrally tune in the middle-IR region (from 2.5 to 3.5 μm), it was possible not only to lower the detection limit but also extend the technique to other isotopes such as ^{13}C. For example, they were able to determine isotopic purity of methanol and its ^{13}C and deuterated samples such as $^{13}CH_3OH$, CD_3OH, CD_2HOH, and CDH_2OH at concentrations as low as 10^{-3} % (w/w).[92] Other uses of near- and middle-IR thermal lens for trace characterization include determination of nucleotides (with combined use of an erbium-doped fiber amplifier (EDFA) and an AOTF that can provide tunable near-IR radiation from 1500 to 1570 nm)[93] and determination of phosphorus with NIR diode laser excitation.[48]

The high sensitivity of the thermal lens technique makes it possible to use it to measure higher overtone spectra, which is not possible with dispersive or FTIR instruments. For example, it was possible to measure overtones of C–H stretching vibrations of aliphatic aldehydes, methane, and saturated hydrocarbons up to $\Delta\nu = 7$ in liquid nitrogen and liquid argon detected at concentrations as low as 15 ppm.[94–107] Other results are summarized and tabulated in Table 2.

4.1.5 *Sensitive Determination of Kinetics*

As evident from Equation (4), typical time constants (t_c) in TLS experiments are in the range of milliseconds in liquids and even shorter in gasses, depending also on the focusing of the pump beam. The thermal lens signal is therefore independent of changes in absorbances of the sample, unless such changes occur at times much shorter than the experimental time constant t_c.

When the absorbing species transforms rapidly during the excitation due to some chemical reaction, the changes in absorbance must be considered in theoretical treatment of the thermal lens. On the other hand, this gives the possibility of deducing the reaction rate constants and information on the order of fast chemical reactions. For this purpose, novel theories have been derived to describe the thermal lens signal for reactions of zero, first, and second order.[17]

For example, for the case of zero-order reaction, the following expression, derived on the basis of the aberrant model, indicates decrease in the thermal lens signal due to disappearance of the analyte (the second term on the right-hand side of Equation (10)):

Table 2 Thermal lens measurements in the near- and middle-infrared region

Molecule	References
Overtones of C–H stretching vibrations (up to $\Delta\nu = 7$) of aliphatic aldehydes	94
Overtones (up to $\Delta\nu = 7$) of methane and saturated hydrocarbons in liquid nitrogen and liquid argon were detected with limit of detection of 15 ppm	95–97
Overtones of saturated hydrocarbons dissolved in liquefied Ar, Kr, Xe, and N_2	98
Real-time monitoring of supercritical fluid extraction	99
Overtone of C–H in conjugated resonance structure (e.g. biphenyl)	100
Overtones of methyl, ethyl alcohols, and cyanides	101
Aniline and haloanilines	102
Overtones (up to $\Delta\nu = 6$) of C–H in trichloroethylene	103
Overtones of C–H (up to $\Delta\nu = 5$) in acetophenone and benzaldehyde: aryl and methyl local modes	104
Aryl C–H stretching	105
Overtone of free O–H stretching of $C_nH_{2n+1}OH$ ($n = 2, 3, 4, 6, 10, 14$)	106
Overtones of C–H (up to $\Delta\nu = 5$) in heterocyclic compounds	107
Determination of chemical and isotopic purities in various solvents including water in D_2O and in THF at LOD of 0.006 and 0.3% (v/v) by TLS with near-IR Ti-Sapphire laser excitation	90
Simultaneous determination of water and DMSO-h_6 in DMSO-d_6 and CD_3OH in CD_2HOH and CDH_2OH by TLS with near-IR Ti-Sapphire laser excitation	91
Determination of isotopic purity of methanol and its ^{13}C and deuterated samples ($^{13}CH_3OH$, CD_3OH, CD_2HOH, and CDH_2OH with LODs of 10^{-3} % (w/w) by TLS with F-center laser excitation.	92
Determination of nucleotides by TLS with near-IR erbium-doped fiber amplifier excitation	93
Determination of Phosphorus by TLS with near-IR semiconductor laser excitation	48

$$S = -\frac{2.303PA}{k\lambda}\left(\frac{\partial n}{\partial T}\right)\tan^{-1}\left(\frac{1}{(1+t_c/t)\sqrt{3}}\right) + \frac{2.303PA}{k\lambda}\left(\frac{\partial n}{\partial T}\right)\frac{k_r}{C_0}\left[(t+3t_c/4)\tan^{-1}\left(\frac{1}{(1+t_c/t)}\right) + \frac{t_c\sqrt{3}}{8}\ln\left[\left(1+\frac{t}{t_c}\right)^2 + \left(\frac{t}{t_c\sqrt{3}}\right)^2\right]\right] \quad (10)$$

When the reaction rate constant k_r equals zero, the expression becomes identical to the case with constant concentration of the analyte with initial concentration C_0.

On the basis of the developed theories, computer calculations were performed to simulate conditions for various chemical reactions. A novel thermal lens spectrophotometer, which can be used for simultaneous measurements of thermal lens and transmittance, was constructed to verify the developed theories and to implement the thermal lens technique for sensitive kinetic determinations.[18] The agreement of measured experimental results with the values predicted by the developed theories confirmed that the thermal lens technique provides kinetic results, which are not only accurate and precise but can also be obtained with reagents whose concentrations are about 100 times lower compared to conventional transmission methods.

The applicability of the thermal lens method for studies of fast chemical reactions in solution was further confirmed by investigating the photolabile Cr–DPC complexes in water.[108,109] An abnormal behavior of the thermal lens transient induced by a photochemical reaction was observed during optical excitation (Figure 3).

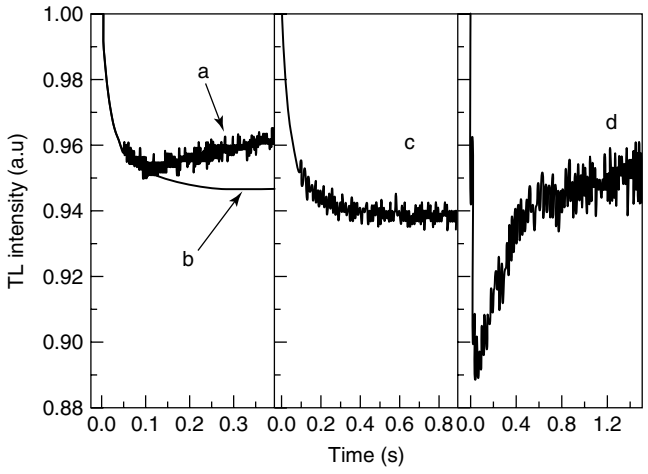

Figure 3 Thermal lens transients for aqueous Cr–DPC solutions ($12\,\mu g\,L^{-1}$ Cr^{VI}) with 100 mW excitation power (trace a) and 300 mW excitation power (trace d). Trace b is the theoretical curve for given experimental conditions. Trace c was generated by the background absorbance of water at 1.1 W excitation power. (Reproduced from Ref. 107. © Elsevier, 1980.)

The existing theoretical model of the thermal lens effect was further generalized in order to take into account the time dependence of the absorbance of the sample due to the changes in concentration resulting from the photochemical reaction as well as from diffusion of absorbing species. The comparison of experimental measurements under different reaction conditions demonstrated the usefulness of the time-resolved thermal lens method for the study of photochemical reactions under the presence of absorbing species diffusion and confirmed its capability of monitoring the processes in a quantitative way and with a temporal resolution of a few milliseconds. The applicability of the technique is however limited by the experimental time constant, which cannot be decreased infinitely by reducing the radius of the pump beam. Other photothermal techniques such as thermally induced grating must be used for investigations of faster chemical reactions occurring on the nanosecond time scale.[110]

4.2 Applications Based on Small-volume Characteristic of Thermal Lens Techniques

4.2.1 Microfluidics

An important milestone in the development of TLS was the introduction of the TLM,[111] which enabled a series of new applications of TLS in microchemical analysis.[9] This stems from the unique geometry of pump and probe beams in TLM, which are aligned coaxially under the microscope and focused with a single chromatic lens. The resulting chromatic aberration of a few micrometers enables pump–probe configuration suitable for the detection of analytes in microwells and microchanels, which cannot be performed on analytical microchips by the transverse mode TLS. In addition, microchips provide a platform for various steps of chemical analysis, such as mixing of analytes and reagents, liquid or solid phase extraction, phase separation, concentration of gaseous analytes, growing of cell cultures, as well as sample heating, which can be performed on-line.[9]

The first demonstration of on-chip chemical determination relying on FIA combined with TLM was based on a microfluidic system consisting of $150 \times 100\,\mu m$ microchannels fabricated on a quartz glass chip, which resulted in the determination of Fe^{II} at an absolute amount of 6 zmol (calculated for a detection volume of 3

fL) after reaction with 1,10-phenanthroline. Solutions of Fe^{II} and the reagent were introduced through separate microchannels and transported into the detection area by a capillary action after mixing in a joint channel by molecular diffusion.[112] Even though the concentration detection limits are not that low (4×10^{-6} M) compared to other TLS methods, the required amount of Fe^{II}, which can be detected in 200 nL of the introduced sample, is only 0.4 pmol, i.e. over 20 times lower than that reported for CE-TLS. This demonstrates that microchip-assisted FIA-TLM is particularly suited for small-volume samples, and can in addition be performed in a relatively short time (about 2–3 min per sample for the given case). Further optimization of the optical-scheme design using presynthesized ferroin indicated that LODs of 1×10^{-8} M can in principle be achieved for the determination of Fe.[9,113]

An on-chip integrated FIA-TLM system, with flow rate ($0.1–0.2\,\mu L\,min^{-1}$) controlled by microsyringe pump, was used for the determination of L-ascorbic acid (AA) and dehydroascorbic acid (DHAA) in urine.[114] Determination of AA is based on the reduction of Fe^{III} by ascorbic acid and subsequent reaction of Fe^{II} with 1,10-phenanthroline. Preparation of samples is simple as the high sensitivity of TLM (for AA the LOD $= 1 \times 10^{-7}$ M, i.e. 1 zmol) requires up to $100 \times$ dilution, which reduces the effect of background absorption from colored samples (urine) to negligible levels. Determination of DHAA, however, requires the reduction to AA by dithiothreithol (DTT) before injection of the sample, and the concentration of DHAA is determined from the difference in AA concentration in oxidized and original sample. The method was applied for the analysis of vitamin C tablets as well. Another application of FIA-TLM for analysis of pharmaceuticals was the determination of catecholamines (LOD = 2 zmol for epinephrine, nor-epinephrine, dopamine, and L-dihydroxyphenylalanine) by using on-chip coloring oxidation to aminochromes by sodium metaperiodate, which required only 15 s for completion.[115]

The next important innovation in the evolution of TLM for microfluidic systems was the integration of the extraction step into analytical procedures for the determination of metal ions and other analytes. This is not only important for the improvement of sensitivity through higher enhancement factor of organic solvents but also for higher specificity of the determination and removal of interferences. Such procedures on a microchannel chip were, for example, developed for the determination of uranyl ions (U^{VI}) after their direct extraction from aqueous solution into tributylphosphate.[116] Other metal ions (Pb^{II}, Co^{II}, Cu^{II}, Fe^{II}, Ni^{II}, K^+, Na^+) can be extracted after their complexation with ligands or by ion pairing providing various degrees of selectivity.[117–120] The advantage of performing the extraction in a microspace of a microchannel is the large specific area of liquid–liquid interface and short diffusion distance, which provides high extraction yields in times 1 order of magnitude shorter compared to extraction using separatory funnels and mechanical shaking. The combined effect of efficient extraction and high enhancement factors in organic liquids resulted in extremely low limits of detection, which are most impressive for the determination of lead as Pb^{II} octaethylporphyrin after extraction into benzene.[117] The reported LOD of about 1×10^{-10} M corresponds to the average presence of less than one molecule (0.4) of the analyte in the probed volume (7.2 fL) within the measurement time (0.1–1.0 s). Additional selectivity can be introduced by intermittent introduction of different organic solvents into a microchannel with a single aqueous phase containing various analytes. This was demonstrated for the case of Na^+ and K^+ ions by their sequential extraction into organic solvents containing a lipophilic indicator (KD-A3) common to both ions, and different ion-selective neutral ionophores (valinomycin and DD16C5).[119] The reported response time and the minimum required reagent solution for on-chip ion-sensing system were about 8 s and 125 nL, respectively, indicating the advantages of the microchip chemistry. Another approach to improved selectivity is also selective degradation of complexes formed by nonselective ligands. This was achieved by exploiting the methodology of continuous-flow chemical processing based on the combination of microcircuit operations and a multiphase flow network.[120] Such a methodology enables complexation of Co^{II} and other metal ions by 2-nitroso-1-naphthol and their subsequent extraction by *m*-xylene in a continuous-flow operation. In the next stage, the organic phase is separately brought in contact with aqueous HCl and NaOH in a microchannel in order to decompose the interfering chelates of Cu^{II}, Fe^{II}, and Ni^{II} and wash them out of the organic phase where Co^{II} can be determined free of interferences at the 0.13 zmol level (1.8×10^{-8} M).

Recently, a micro-multiphase laminar flow on a microchip was also applied for the determination of organic compounds such as carbamate pesticides (carbaryl, carbofuran, propoxur, and bendiocarb).[121] The multichannel microchip enabled hydrolysis of carbamates to corresponding naphthols, their diazotization by trimethylaniline or *p*-nitrobenzenediazonium fluoroborate, and extraction into toluene or 1-butanol, where the derivatives were detected by TLM with LOD values as low as 1.1×10^{-8} M, as demonstrated for carbofuran.

The versatility of microchip-based TLM detection offers many other interesting configurations for assays such as microchip-based micro-ELISA applied, for

example, for the determination of interferon(IFN)-γ,[86] and a TLM method for monitoring of intercellular messengers such as arachidonate.[122] In the first case, the polystyrene microbeads precoated with the IFN antibody were placed into a microchip channel. 0.1 ng mL^{-1} (6 pM) of IFN could be detected by the TLM-micro-ELISA procedure. Monitoring of the arachidonate released from the rat nerve cells, kept in a 0.1-mm-deep, 1-mm-wide, and 10-mm-long culture chamber on a microchip, was however much simpler, and required only the injection of glutamate, which is a known neurotransmitter. This stimulated the release of the retrograde messenger (arachidonate), which was detected by TLM at 1.3×10^{-5} M concentration (for injection of 10^{-4} M glutamate) corresponding to 1.3 fmol of arachidonate released per cell.[122]

Microchip ELISA was also used for the detection of secretory human immunoglobulin A (s-IgA), which was initially adsorbed on polystyrene beads placed in a microchannel of a glass chip. The secondary antibodies (anti-s-IgA) were in this case conjugated with colloidal gold and after their interaction with s-IgA on polystyrene beads, the TLM quantification of 1 μg mL^{-1} of s-IgA was possible.[123] Owing to the 37× reduced sample volume/sorbent surface ratio in a microchip, as compared to microtiter plates in conventional ELISA tests, the antigen–antibody reaction was completed in 10 min as deduced from the stabilization of TLM signal. This represents a substantial improvement in sample throughput compared to over 15 h required for the conventional bulk scale ELISA and enables sensitive determination of s-IgA in saliva, where concentrations are normally on the order of 200 μg mL^{-1}. Colloidal gold conjugated antibodies of immunoglobulin G (IgG) were used for the detection of carcinoembryonic antigen (CEA) in human sera – a commonly used marker of colon cancer.[89] In this case, the assay requires sequential addition of two antibodies (rabbit anti-CEA and colloid gold conjugated IgG), following the binding of CEA to a mouse anti-CEA antibody adsorbed on polystyrene beads. Still, the entire assay can be completed in 35 min (compared to 45 h with ELISA on microtiter plates) with the detection limit of 0.03 ng mL^{-1} CEA, which enabled assays of patient's sera with CEA concentrations in the range of 0.67–7.3 ng mL^{-1}.

An application of the TLM system for two-dimensional monitoring of cytochrome c distribution in a neuroblastoma-glioma hybrid cell cultured in the microflask (1 mm ×10 mm ×0.1 mm; 1 μL) fabricated in a glass microchip was also described.[88] Cytochrome c release from mitochondria to cytosol during the apoptosis of the cell was successfully monitored with a 1 μm resolution, after addition of staurosporin, which triggered the apoptosis. The absolute amount of cytochrome c detected in the probed volume was estimated to be about 10 zmol. A further important step in the application of TLS for studies of single cells was achieved by the detection and measurement of human leukocyte antigens (HLA) on the surface of a single blood cell.[82] Antigens of HLA-A, -B, and -C loci on the lymphocytes were identified and quantified by TLM and an image of HLA-A, -B, and -C antigen distribution on a mononuclear leukocyte was obtained (1.5–2 μm resolution). For this purpose, anti-HLA-A, -B, and -C antibodies were labeled with colloidal gold and added to mononuclear leukocytes for incubation before being assayed. The TLM laser microscope was specially devised for measuring convex surface cells, which are 9–12 μm in diameter, and the deviation of the TLM focal point from the cell surface was corrected by utilizing the phase of the signal.

4.2.2 Capillary Electrophoresis

Capillary electrophoresis is another example of the advantageous use of TLS as a highly sensitive technique in which TLS can overcome the problem of short optical pathlength and small-volume samples, governed in CE by the dimensions of capillaries. Compact TLS detector systems were developed for applications in CE-TLS,[124] which rely on transversal TLS configuration as capillary electrophoresis requires probing of volumes on the order of some 10 pL. The capability of TLS to probe small-volume samples is indeed exploited the best in capillary electrophoresis, where TLS enables direct detection in capillaries with inside diameters 50–250 μm, without a need of a detection cell. Even smaller volumes can be probed by the use of TLM. However, the curved surface of the capillary reduces the sensitivity as well as the reproducibility of the TLM technique, which requires an interface chip for coupling CE with TLM detection.[125] This might be the main reason why TLM did not find real application in chemical analysis by CE, but was most frequently used for microfluid analysis on microchemical chips.

Application of TLS detectors in capillary electrophoresis (Table 3) resulted in the determination of 1.8×10^{-7} M dabsylated arginine, histidine, leucine, alanine, glycine, and glutamic acid in a detection volume of 50 pL.[126] By taking into account very small detection volume, a detection limit of 10 amol was calculated, which represents a 20-fold improvement compared to previous applications of CE-TLS for detection of dabsylated amino acids. In part, the low LODs are due to the addition of 15% of methanol and 1% THF to the solvent in order to improve the separation efficiency and reduce the retention times to less than 11 min. Furthermore, the added organic solvents also improve thermo-optical properties of the sample medium, thereby increasing the signal-to-noise ratio and lowering the LOD values.

Table 3 Some applications of TLS detection in ion chromatography and capillary electrophoresis

Analyte	Excitation	Coloring reagent	LOD	References
Fe^{II}, Fe^{III}	Ar laser 514.5 nm, 100 mW	1,10-phenanthroline	$5\,\mu g\,L^{-1}$	55
Cr^{VI}, Cr^{III}	Ar laser 514.5 nm, 160 mW	DPC	$0.1\,\mu g\,L^{-1}$ $10\,\mu g\,L^{-1}$	57
Cu^{II}, Zn^{II}, Pb^{II}, Cd^{II}, Co^{II}, Ni^{II}	Ar laser 514.5 nm, 95 mW	PAR	$4–5\,\mu g\,L^{-1}$ (for Co^{II} and Cu^{II})	58
K^+, Cu^{2+}, Al^{3+}	He–Ne, 632.8 nm, 18 mW	Methylene blue (indirect detection)	2.1×10^{-7} M ($S/N = 2$)	127
Lysine	He-Ne, 632.8 nm, 20 mW	Methylene blue (indirect detection)	7.5×10^{-7} M	128
Amino acids	Ar laser 458 nm, 150 mW	DABSYL	1.8×10^{-7} M	126
Amino acids	KrF laser 248 nm, 10 μJ	PTH	$1.4–4.8 \times 10^{-7}$ M	129
Tamoxifen + metabolites	KrF laser 248 nm, 10 μJ	Direct detection	10^{-7} M	130
Etoposide, etoposide phosphate	Frequency-doubled Ar laser 257 nm	Direct detection	$100\,\mu g\,L^{-1}$ $170\,\mu g\,L^{-1}$	131
Alkyl-sulfonic acids	He–Cd laser 325 nm, 50 mW	Mordant yellow 7 (indirect detection)	$4–7 \times 10^{-7}$ M	132
Chloramphenicol, dichlofenac, pentoxifyllin, oxprenolol	Ar laser 514.5 nm	Reactive red (indirect detection)	4.5×10^{-7} M	59

The advantage of using larger fractions of organic solvents in separation buffers was further demonstrated by determination of 17 different phenylthiohydantionated (PTH) amino acids (PTH-amino acids) injected onto the capillary.[129] PTH-amino acids are produced as the end product of the Edman degradation reaction. Using a pulsed KrF excimer laser (248 nm) for excitation, 13 PTH-amino acids were separated with nearly baseline resolution in 14 min and with LODs from 1.6 to 4.8×10^{-7} M. Compared to previously reported results on CE-TLS determination of PTH-amino acids, this method represents an improvement in LOD by an order of magnitude, which mainly can be attributed to the higher thermo-optical enhancement resulting from high acetonitrile content.

High enhancements were fully exploited in nonaqueous CE-TLS, which was first reported for the determination of a nonsteroid antiestrogen tamoxifen and its acid hydrolysis products,[130] which form after ingestion in stomach and may increase the risk of endometrial cancer and blood clots. Unfortunately, no detailed study was performed on the sensitivity and LOD of the method. It is however evident from the presented results that tamoxifen and seven degradation products can be detected at 10^{-7} M level when a 3 : 7 v/v acetonitrile–methanol with 20 mM ammonium acetate was used as a separation buffer.

The only real application of CE-TLS for the analysis of complex samples was recently reported for determination of etoposide and etoposide phosphate in blood plasma.[131] The method based on micellar electrokinetic chromatography allows baseline separation of analytes of interest and potential interfering matrix constituents within 4 min. The reported LODs of $100\,\mu g\,L^{-1}$ for etoposide phosphate and $170\,\mu g\,L^{-1}$ for etoposide represent a 60-fold improvement compared to commercial absorption spectrometric detector operating at the same wavelength (257 nm).

Indirect detection of analytes can as well be exploited in CE-TLS to avoid the problem of weakly absorbing analytes and lack of excitation lasers with wavelengths matching the absorption maxima of detected species. This concept has recently found application in CE-TLS for the determination of various alkyl-sulfonic acids.[132] By applying 50 μM Mordant Yellow 7 azo dye as the background ion, detection of analytes was possible at 325 nm He–Cd laser line, and the limits of detection of 7×10^{-7} M 1-propanesulfonic acid were reported in aqueous buffer (5 mM tris) as separation electrolyte. The LODs were reduced to 4×10^{-7} M by adding 20% (v/v) acetonitrile into the separation electrolyte.

Comparison of some other published results demonstrates that in terms of LODs the indirect TLS cannot compete with direct TLS detection, where such a detection mode is possible. For example, indirect photothermal detection of metal ions, such as K^+, Cu^{2+}, and Al^{3+} in capillary zone electrophoresis with Methylene Blue as background absorber, provides LODs of 3×10^{-7} M as can be recalculated for S/N ratio of 3.[127] This is almost 20 times higher compared to CE-TLS determination of iron ions in rain water with 1,10-phenanthroline as a chromogenic reagent.[133] Large differences in LODs between

direct and indirect detection in CE-TLS can also be found for detection of lysine.[128] In this case, the LOD of 7.5×10^{-6} M (recalculated for $S/N = 3$) was reported for indirect CE-TLS using Methylene Blue and a 20 mW He–Ne laser as the excitation source (632.8 nm). This is again over an order of magnitude higher (20–50 times) compared to direct CE-TLS detection of PTH derivatized lysine and other amino acids.[129]

4.3 Determination of Thermal and Physical Properties of Solvents

In addition to sensitive detection of trace chemical species, it is also possible to use the thermal lens technique as an accurate and sensitive method for the determination of the thermal physical properties of solvents, namely, their dn/dT and thermal conductivity, k, values. These two thermal physical properties can be individually determined by measuring the transient of the thermal lens. This is because, as mentioned earlier, the thermal lens, when recorded as the time-dependent change in the far field beam center intensity ($I_{bc}(t)$) after the onset of excitation laser illumination ($I_{bc}(0)$), is given by Equation (7). The thermal time constant t_c, which depends on the spot size, ω, of the excitation beam in the sample, the density, ρ, specific heat capacity C_p, and thermal conductivity, k, of the solvent, is given by

$$t_c = \frac{\omega^2 \rho c_p}{4k} \tag{11}$$

Thus, θ and t_c values can be obtained by nonlinear curve fitting of the thermal lens transient to Equation (7). Substitution of the t_c value into Equation (11) yields either the thermal conductivity or the heat capacity of the sample. The dn/dT value can then be calculated from Equation (8) using the θ and k values. The accuracy of the method can be evaluated by performing the thermal lens measurement on a solvent whose thermal conductivity, density, and specific heat capacity values are known and comparing the t_c values obtained by thermal lens method with the literature values.

The dn/dT and k values of various solutions including aqueous and organic solvents such as methanol, carbon tetrachloride, chloroform, DMF, DMSO, and heptane were accurately determined by using this method.[134] In addition to their scientific and technological importance, the obtained dn/dT and k values can provide insight into the structure of solutions. As described in the following sections, the thermal lens technique can be successfully used to determine the effect of the temperature on the structure of water, with or without additives such as electrolytes and surfactants.

4.3.1 Thermal Physical Properties of Water

From the study of the temperature effect on thermal lens measurements in water, it was found that the magnitude and sign of the thermal lens signal intensity are strongly dependent on the temperature of the aqueous solution.[135,136] As shown in Figure 4, depending on whether the measurements are performed at temperatures lower or higher than −0.01 C, the photoinduced thermal lens can have either a positive (converging) or negative (diverging) focal length. At precisely -0.01 ± 0.04 C, no thermal lens signal could be observed. This is because the dn/dT values of water are positive at $T < -0.01$ C, negative at $T > -0.01$ C, and equal to zero (i.e. maximum refractive index) at $T = -0.01$ C.[135,136]

These results are of particular interest considering the fact that water exhibits maximum density at +4.0 C, which is different from the temperature at which its refractive index is maximum. This behavior is distinctly different from other liquids that are known to undergo

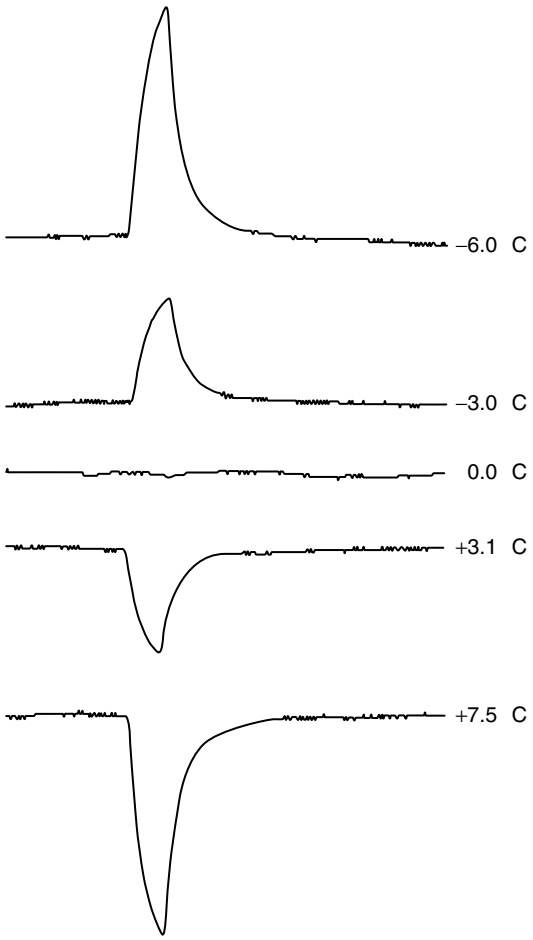

Figure 4 Thermal lens signals of aqueous solution at different temperatures.

maximum density and refractive index at the same temperature. The Lorentz–Lorenz equation relating refractive index n and density ρ for liquids has been used to explain this behavior[135]:

$$\frac{n^2-1}{n^2+2} = \rho P \tag{12}$$

where P is the specific refraction. For most liquids, P is generally assumed to be constant and independent of pressure and temperature. However, this assumption is not valid for water as it was theoretically[135] and experimentally[136] proven that P does vary slightly with both of these variables. Differentiating Equation (12) under this condition, at constant pressure, gives

$$\frac{6n}{(n^2+2)^2}\frac{\partial n}{\partial T} = \frac{\partial P}{\partial T}\rho + \frac{\partial \rho}{\partial T}P \tag{13}$$

It is thus clear that for water the refractive index and density do not go through maxima at the same temperature. Furthermore, because P and ρ are positive and $\partial P/\partial T$ is negative,[135] $\partial n/\partial T$ is expected to go through zero at the temperature where $\partial \rho/\partial T$ is positive, i.e. at temperature lower than 4 C. This prediction is in very good agreement with the results obtained with thermal lens measurements, namely, the refractive index of water undergoes maximum at −0.01 C, whereas its maximum density is at 4 C. A number of explanations have been proposed to explain for the variation of P with temperature and pressure. They include the change with temperature of either the concentration of the ''ice-like'' structure or the average polarizability of water molecules.[135,136]

This unique behavior of water has been exploited in other types of photothermal techniques for measurements, which otherwise is not possible. For instance, it has been demonstrated that by measuring of aqueous solutions of biopolymers at −0.01 C, where dn/dT of water is zero, it was possible to remove the signal due to dn/dT from the total thermal lens signal, thereby enabling the determination of change in volume or the conformation of polymers induced by temperature change.[137] Conversely, by measuring thermal lens signal at +4.0 C, where the density of water is maximum, it was possible to eliminate the contribution due to the change in volume (of aqueous solution) with temperature, which as a consequence makes it possible to measure the change in concentration of solution as a function of temperature.[138]

Using the method described above, the k and dn/dT values of water at different temperatures were obtained from the corresponding thermal lens transient signals. The results are shown in Table 4.[139,140] As listed, within experimental error, the k value remains constant at different temperatures. The dn/dT value, however, undergoes significant change as the temperature varies. Increasing temperature leads to an increase in the dn/dT value. For instance, increase in the temperature by 16 (from 1.26 to 17.98 C) leads to a 14-fold increase in the dn/dT value.[139–141] This observation can be explained in terms of the structure of water. Specifically, it is known that the structure of water is known to be greatly affected by the temperature of the solution. Increasing the temperature of the aqueous solution has the ''hydrogen bond breaking effect''.[139–141] As a consequence, the water has less hydrogen bonds, becomes less structured (or less ordered), and hence can have large changes in the density and in the refractive index with temperature (i.e. higher $d\rho/dT$ and dn/dT values).

Table 4 Thermal conductivity and dn/dT values of water at different temperatures, measured by the thermal lens technique. (Reproduced from Ref. 134. © American Chemical Society, 1988)

Temperature (C)	Thermal conductivity (mW cm^{-1} K^{-1})	dn/dT (10^{-5}, K^{-1})
+19.77	–	–
+17.98	6.1 ± 0.1	−8.6 ± 0.2
+16.13	6.1 ± 0.1	−7.4 ± 0.2
+14.31	6.1 ± 0.1	−8.6 ± 0.2
+12.52	6.1 ± 0.1	−6.7 ± 0.2
+10.68	5.9 ± 0.1	−5.8 ± 0.1
+8.86	5.8 ± 0.1	−4.8 ± 0.1
+7.13	5.9 ± 0.1	−4.0 ± 0.2
+5.15	5.7 ± 0.1	−2.8 ± 0.1
+3.34	6.0 ± 0.1	−1.7 ± 0.1
+1.26	5.3 ± 0.1	−0.6 ± 0.1
−0.76	7 ± 2	+0.4 ± 0.1
−2.60	5 ± 1	+1.3 ± 0.3
−4, 47	5.3 ± 0.4	+2.2 ± 0.2
−6.78	5.4 ± 0.2	+3.6 ± 0.1
−8.84	5.6 ± 0.1	+5.1 ± 0.2

4.3.2 *Thermal Lens Studies of the Effects of Surfactants and Electrolytes on Structure of Water*

The thermal lens technique has also been successfully used to determine the effects of electrolytes and surfactants on the structure of water.[139–141] It has been reported, based on the IR, Raman, and NMR studies, that adding certain electrolytes or surfactants into water has the same effect as heating up the solution.[139–141] It is expected, therefore, that thermal lens signal of water will be modified when such compounds are added. It was found that electrolytes provided up to a twofold enhancement in the thermal lens signal.[139–141] Higher enhancement (up to eightfold) was also achieved when surfactants were added to the solution.[139–141] Interestingly, micellization does not seem to have any

observable effect on the enhancement. In both the cases, it was found that the enhancement was not due to the effect of the electrolyte on the thermal conductivity but rather on the dn/dT of the solution. Interestingly, the effect of electrolytes and surfactants seems to be different from the temperature effect.[139–141] This conclusion was derived when the change in dn/dT upon the addition of electrolytes or surfactants was deconvoluted into two parts. The first, which results from the difference in the specific refractivity and dn/dT of the electrolyte or surfactant solution as compared to that of pure water, has a stronger effect on the enhancement than the second, which is caused by the alteration of the hydrogen-bonding network of water.[139–141]

4.4 Dependency of Thermal Lens Signal on Thermo-Optical Properties of Sample Matrix and Its Utilization to Enhance Sensitivity

For weak absorbing species, the thermal lens signal that is measured as the relative change in the beam center intensity in the far field, $\Delta I_{bc}/I_{bc}$, is given by

$$\frac{\Delta I_{bc}}{I_{bc}} = \frac{-2.303P(dn/dT)A}{1.91\lambda k} \tag{14}$$

where λ is the wavelength of the probe beam.

The relative change in the beam intensity, when determined by conventional absorption techniques for a weakly absorbing species having absorbance A, is

$$\frac{I_0 - I}{I_0} = 1 - 10^{-A} = 2.303A \tag{15}$$

It is therefore clear from Equations (14) and (15) that the sensitivity of the thermal lens technique is relatively higher than that of conventional absorption methods. The sensitivity enhancement factor E is calculated from Equations (14) and (15) to be

$$E = \frac{-P(dn/dT)}{1.91\lambda k} \tag{16}$$

It is evidently clear from Equation (16) that the sensitivity of the thermal lens technique is not only directly proportional to the excitation laser power P but also depends on the thermal physical properties of the solvent used. Generally, nonpolar solvents are good media for thermal lens measurements owing to their high dn/dT and low k values.[134,142,143] Water, which is the universal solvent for biochemical and biological samples, is the worst medium for thermal lens technique because it has a very low dn/dT and high k values. In fact, it has been calculated and experimentally verified that, at the same laser intensity, thermal lens measurements in CCl_4 and n-pentane are 38 and 40 times higher than those in water.[134,142,143] The dependency of the thermal lens signal on the thermal physical properties of solvent can, in principle, be exploited to enhance the sensitivity and selectivity of the technique. Organized assemblies such as micelles, reversed micelles, and crown ethers can be effectively used to modify the thermal physical properties, (i.e. dn/dT and k values) of the medium that, in turn, enhances the sensitivity of the thermal lens measurements. Sensitivity enhancement through manipulation of thermal physical properties of the medium can also be achieved by use of room temperature ionic liquids or by changing measurement temperature of aqueous solutions. All of these enhancement methods are described in the following sections.

4.4.1 Sensitivity Enhancement by Aqueous Micelles

Aqueous micelles have been found to enhance the thermal lens of solubilized substrates.[142] The enhancement depends on the type of micelles and the structure of the substrate.[142] The highest enhancement was achieved when there were strong interactions between the micellar aggregate and the substrate. For instance, compared to that in water, the thermal lens enhancement provided by a nonionic surfactant such as hexaethylene glycol mono-*n*-dodecyl ether ($C_{12}E_6$) was only 2.3 times for 9-nitroanthracene but up to 7 times for 11-(9-anthroyloxy) undecanoic acid (ANU).[142] It was suggested that the long hydrocarbon tail in ANU makes it possible for this compound to interact strongly with the nonionic micelles, which, as a consequence, leads to a higher thermal lens enhancement. While it is possible to achieve enhancement in the thermal lens signal by use of aqueous micelles, the enhancement factor in all cases has never exceeded 10× relative to that in pure water. This is lower than the enhancement achieved in reversed micellar media as described below. A number of reasons might account for this difference, but the most likely one is due to the difference in the respective enhancement mechanisms. Aqueous micelles increase the thermal lens signal of a solubilized substrate because, as explained in the previous section, the surfactant molecules are known to modify the specific refractivity and dn/dT of the solution as well as to alter the hydrogen bond networks of water. This, according to Equation (16), leads to an increase in the thermal lens signal. While surfactant molecules can change properties and structure of water, they cannot, however, completely change it to an environment similar to that of a nonpolar solvent. Thus, it is hardly surprising that the enhancement provided by aqueous micelles is relatively lower than those observed for reversed micelles.

4.4.2 Sensitivity Enhancement by Reversed Micelles

Table 5 shows the effects of solvents and reversed micelles on the thermal lens signal intensity of terbium chloride.[134] The lanthanide ion was chosen because of its high hydrophilicity, namely, it is very soluble in water, sparingly soluble in polar solvents, and insoluble in nonpolar solvents.[134] As expected, the thermal lens signal amplitude of Tb^{3+} in methanol is 10 times higher than that in water. The enhancement is further increased to 15 times when Tb^{3+} is in 1-butanol. Substantial enhancement was found, however, when Tb^{3+} is solubilized in AOT reversed micelles. Sodium bis(2-ethyl hexyl) sulfosuccinate or Aerosol-OT (AOT) was used to investigate the effect of reversed micelles because this anionic surfactant can form reversed micelles in a variety of nonpolar solvents and can solubilize large amounts of water.[134]

It is interesting to note that, in spite of the fact that the Tb^{3+} ions are soluble in the water pool of the reversed micelles, the thermal lens signal intensities of the Tb^{3+} are much higher than those in pure water. The enhancements were found to be dependent on the particular nonpolar solvent in which the reversed micelles are formed. Under identical conditions, Tb^{3+} was found to exhibit 38-fold enhancement when it is solubilized in AOT/CCl_4 reversed micelles as compared to that in pure water. The enhancement factor decreases to 23 in AOT/*n*-pentane, 20 in AOT/cyclohexane, 21 in AOT/*n*-heptane, and 15 in AOT/nonane.[134]

Taking advantage of the fact that AOT forms reversed micelles in dioxane[138] and terbium chloride is soluble in this solvent, thermal lens measurements were also performed for Tb^{3+} in pure dioxane and for Tb^{3+} solubilized in the water pool of AOT/dioxane reversed micelles. The thermal lens of Tb^{3+} in pure dioxane is 22 times more than that in pure water and is the same, within experimental error, with that of Tb^{3+} in AOT/dioxane (25×; Table 5). These results clearly demonstrate that the surfactant molecules do not produce an observable effect on the dn/dT and k values of the dioxane solution. Additional information can be obtained from the relative thermal lens signal intensity of Tb^{3+} in AOT/CCl_4, AOT/hydrocarbons, and AOT/cyclohexane reversed micellar systems compared to that in pure water. It is known that AOT forms its largest reversed micelle in cyclohexane as the aggregation number, N, in this solvent is between 45 and 65.[134] Medium-sized micelles can be found in hydrocarbons ($N = 25–31$) with the CCl_4 providing the smallest ($N = 17$).[134] Any micellar effect, if existent, is expected to provide a larger enhancement for the medium leading to large-sized micelles, whereas smaller enhancements are expected for the smaller size micelles. However, the observed enhancement values are in the reversed order: AOT/CCl_4 > AOT/hydrocarbons > AOT/cyclohexane.

Table 5 Relative thermal lens signal intensity of $TbCl_3$ in different media. Taken from Tran[134]

Surfactant	Solvent	(Relative intensity)$_{exptl}$	(Relative intensity)$_{calcd}$
–	Water	1	1
–	Methanol	10	17
–	1-Butanol	15	21
–	Dioxane	22	27
AOT	Dioxane	25	27
AOT	*n*-Nonane	15	28
AOT	*n*-Heptane	21	33
AOT	*n*-Pentane	23	40
AOT	Cyclohexane	20	36
AOT	CCl_4	38	47
SDS	Water	1	1
CTAB	Water	1	1

Information of the micellar effect on the thermal conductivity, k, is relatively scarce and inconclusive. In the absence of aggregation such as that for AOT in CCl_4 without any solubilized water, the surfactant had no observable effect on k because the k values were found to be the same with and without the surfactant.[134] Adding water to the solution leads to the formation of AOT reversed micelles in CCl_4.[134] The thermal conductivity of the mixture was found to be dependent on its chemical composition.[138] The results suggest that, at low solubilized water concentration, the k value for the mixture is higher than that for the pure CCl_4 solution.[138] This, according to Equation (16), would result in lowering of the thermal lens signal intensity. Because the observed thermal lens signals were, in fact, enhanced by AOT/CCl_4 reversed micelles, the reversed micellar effect on the k value of the solution is very small at low solubilized water concentration.

Collectively, these results suggest that the effect of the reversed micelles on the dn/dT and k values of the bulk nonpolar solvents is rather small. The thermal lens signal magnitude of Tb^{3+} in AOT reversed micellar systems is governed mainly by the thermo-optical properties of the nonpolar solvent even though the metal ions are solubilized in the water pool.

4.4.3 Sensitivity Enhancement by Crown Ethers

It was demonstrated recently that by using crown ethers as the extractant, it was possible to enhance not only the sensitivity but also the selectivity of the thermal lens detection of such metal ions as lanthanide ions.[143] This is because crown ether (host) can selectively form an inclusion complex with a metal ion (guest) and this complex formation will introduce the hydrophobicity into the analyte (i.e. metal ion).

As a consequence, the complex is extracted from the thermo-optically poor water into a nonpolar solvent that has relatively better thermo-optical properties. The thermal lens signal intensity of the extracted inclusion complexes is expectedly higher than that in pure water. The selectivity enhancement in this case would depend on the size selectivity of the macrocyclic host, i.e. the formation of inclusion complexes between the crown ethers such as 18-crown-6, 15-crown-5, and 12-crown-4 and the lanthanide ion can only be achieved when the size of the metal ion is comparable to the cavity size of the crown ether.[143] For instance, it was shown that by using 15-crown-5, Nd^{3+} ion was extracted from aqueous solution into organic phase such as ethyl acetate, heptanol, octanol, 1,2-dichloroethane, methylene chloride, and chloroform.[143] Compared to that in water, the thermal lens signal intensity of Nd^{3+} was found to be substantially higher when it was extracted into the organic phase: up to 24-fold enhancement was observed in dichloroethane, 20 × in $CHCl_3$, 18 × in CH_2Cl_2, 14×, 13× and 11 × in octanol, heptanol, and ethyl acetate, respectively.[143]

The enhanced selectivity (i.e. selective extraction) was observed when a series of lanthanide ions ranging from Pr^{3+} to Er^{3+} were extracted from the aqueous phase into the organic phase using different crown ethers, namely, 12-crown-4 (12-C-4), 15-crown-5 (15-C-5), and 18-crown-6 (18-C-6). It was found that only small amounts of lanthanide ions (between 8 and 12%) were extracted into the chloroform phase when 12-C-4 was used as the extracting agent. The low extraction yields were probably due to the mismatching in the sizes of the crown ether and the lanthanide ions, i.e. the cavity of 12-C-4, which is between 1.2 and 1.5 Å, was too small to accommodate the lanthanide ions whose ionic diameters were between 1.76 and 2.02 Å.[143] Substantial improvement in the extraction yield was observed when 15-C-5 or 18-C-6 was used as the extracting agent. For instance, up to 39 and 41% of Er^{3+} ions can be extracted from the aqueous phase into the chloroform phase with the use of 15-C-5 and 18-C-6, respectively. The enhancement in the extraction yield was probably due to the fact that the cavities of these crown ethers were sufficiently large (the cavities of 15-C-5 and 18-C-6 were 1.7–2.2 and 2.6–3.2 Å, respectively)[143] to accommodate the lanthanide ions and thus enabled them to be selectively extracted into the organic phase.

4.4.4 *Sensitivity Enhancement by Room Temperature Ionic Liquids*

As described above, nonpolar, volatile organic solvents (e.g. benzene, hexane, and CCl_4) should provide good media for thermal lens measurements owing to their high dn/dT and low k values. Conversely, water and polar solvents are poor media as they have low dn/dT and high k values. This is very unfortunate because it limits the utilization of the thermal lens technique as water, in addition to its nonpolluted properties, is the most widely used solvent. As a consequence, considerable efforts have been made either to develop novel solvents that have better thermo-optical properties than water but do not produce pollution like traditional volatile organic solvents. It is expected that room temperature ionic liquids (RTILs) with their unique properties (nonvolatile, no vapor pressure, high solubility power, adjustable polarity) should serve as a greener solvent but with higher sensitivity for thermal lens measurements.[144]

Tran and coworkers have successfully demonstrated that RTILs can be used as attractive and superior solvents for thermal lens measurements.[145] RTILs are superior to water as they have relatively high solubility power and, by judiciously selecting either the cation and/or anion, they can dissolve many different types of compounds including polar as well as nonpolar compounds. More importantly, RTILs provide a relatively better medium for thermal lens measurements than water. The authors show that not only do the RTILs offer at least 20 times higher sensitivity than water but that the enhancement can be appropriately adjusted by changing either the cation and/or the anion of the ILs.[145] For example, the sensitivity in $[BMIm]^+$ $[Tf_2N]^-$ is about 26 times higher than that in water. It can be increased up to 31 times by changing the anion to $[PF_6]^-$ (i.e. $[BMIm]^+$ $[PF_6]^-$) or up to 35 times by changing the cation to $[OMIm]^+$ (i.e. $[OMIm]^+$ $[Tf_2N]^-$). [145] In fact, the sensitivity of thermal lens measurements in RTILs is comparable to those in volatile organic solvents such as benzene, carbon tetrachloride, and hexane, but RTILs are more desirable as they have virtually no vapor pressure. As described in the previous section, the thermal lens technique is particularly suited as the detection method for microfluidic devices because it has high sensitivity and small-volume capability (conventional spectrophotometric technique cannot be used for such devices because not only does it have much lower sensitivity but also its sensitivity is proportional to the pathlength of the sample). The RTILs induced thermal lens enhancement reported here can, therefore, be synergistically used in microfluic devices by simply replacing either water (to enhance detection sensitivity) or the VOC solvent (to prevent pollution and also to enhance the sensitivity) with ILs.

4.4.5 *Sensitivity Enhancement by Exploiting Unique Properties of Water*

As described in the previous section, the magnitude and sign of the thermal lens signal intensity were found to be strongly dependent on the temperature of the aqueous solution. Depending on whether the measurements are

performed at temperatures lower or higher than −0.01 C, the photoinduced thermal lens can have either a positive (converging) or a negative (diverging) focal length. At precisely -0.01 ± 0.04 C, no thermal lens signal could be observed.[135,136] This is because the dn/dT values of water are positive at $T < -0.01$ C, negative at $T > -0.01$ C, and equal to zero (i.e. maximum refractive index) at $T = -0.01$ C.[135,136] This unique characteristic was exploited to enhance the sensitivity of thermal lens measurements in water. For instance, the thermal lens signal of an aqueous solution was enhanced up to 2.4 times when the temperature of the solution was increased from +20.0 to +90.0 C.[136] For thermally unstable compounds, the sensitivity enhancement was achieved by synergistic use of the bimodal characteristic of the thermal lens technique and the temperature effect on the thermo-optical properties of water. Typically, two sample cells, one at −7.9 C and the other at +12.0 C, were placed on both sides and symmetrically about the beam waist. It was found that the sensitivity of this two-cell system was 1.80 or $(1 + T)$ time to that of the single cell (T is the transmittance of the first cell).[136]

5 CONCLUSIONS

In summary, it has been demonstrated that the advantages of the thermal lens techniques are not only limited to their ultrasensitivity but also include other unique features that no other techniques have, namely, their small-volume sample capability and their dependency on thermo-optical properties of solvents. Because of these unique features, thermal lens techniques have been very popular as they can be used for measurements and studies, which is otherwise impossible using other existing techniques. However, it would be misleading to conclude this article with the idea that the thermal lens technique has instrumentally reached maturity and that it does not have disadvantages and defects. In fact, even now, the field has not been fully developed. Disadvantages and defects do exist, and much research needs to be performed to further improve the selectivity and applicability and to make it easier to operate and maintain the instrument. Some of the possible improvements are discussed below.

A light source with Gaussian distributed intensity is essential for excitation. As a consequence, instruments that have been developed to date are based exclusively on the use of laser as the light source for excitation. Currently, lasers are much more stable and reliable than those in the early days. Unfortunately, even now, lasers are not available for the entire UV–visible, near-, and middle- infrared but rather only for certain wavelengths or narrow spectral tuning ranges. This is unfortunate considering the advantages that the thermal lens techniques can offer. It is, therefore, of particular importance that this restriction be removed or ameliorated. Considerable efforts have been made in the last few years to address this problem. Of particular interest is the fiber lasers and optical amplifiers made by doping fiber with rare earth ions (e.g. erbium-doped fiber amplifier or EDFA), which were developed recently.[146] These lasers are based on the use of fibers doped with rare earth ions including erbium, neodymium, and praseodymium as the lasing media.[93,146,147] As these lasers are pumped by diode lasers, their sizes are much smaller compared to those of gas and solid lasers. However, because fiber as long as several miles can be used, these fiber lasers can provide output power in the range of several watts. These features make them particularly useful for the thermal lens technique, in particular, for the miniaturized thermal lens instruments. While it is true that, because of the strong interest in telecommunication, these doped fiber lasers are currently available only in the near-infrared region, i.e. 1.3 and 1.5 μm, it is, however, expected that other wavelengths, especially those in the ultraviolet and visible regions, will be readily available by doping the fibers with different ions and/or using nonlinear techniques to double, triple, and quadruple the frequency. Other recently developed sources that are attractive in terms of cost are the so-called superluminescence light-emitting diodes. These relatively inexpensive LEDs are now commercially available at many wavelengths in the visible as well as the near-infrared regions. They are potentially suited as excitation sources for thermal lens instruments because they can provide up to milliwatts of CW light, which has a spectral bandwidth of more than 100 nm.[148] As described in the previous section, the AOTF can be used to spectrally tune the wavelength and control the amplitude (i.e. to keep it constant and to turn off the light completely to enable the sample to return to its original thermal state) of the LED. In addition to reducing the cost and complexity of the instrument, such an AOTF-based LED instrument is solid state, contains no moving parts, and is very compact in particular. This undoubtedly would increase the applicability of the instrument. Other notable progress includes recent work,[19] which was described in recent article, on the use of ''hat top'' beam profile for excitation. This work is significant as it enables the use of non-Gaussian beams for excitation.

ABBREVIATIONS AND ACRONYMS

AA	Ascorbic Acid
AChE	Acetylcholinesterase
AO	Acousto-optic

AOTF	Acousto-optic Tunable Filter
CD	Circular Dichroism
CE	Capillary Electrophoresis
CEA	Carcinoembryonic Antigen
CW	Continuous Wave
DABSYL	4-(dimethylamino)azobenzene-4′-sulfonyl chloride
DAD	Diode Array Detector
DHAA	Dehydroascorbic Acid
DPC	1,5-Diphenylcarbazide
DTT	Dithiothreithol
EDTA	Ethylenediaminotetraacetic Acid
ELISA	Enzyme-linked Immunosorbent Assay
ET-AAS	Electro-thermal Atomic Absorption Spectrometry
FFAs	Free Fatty Acids
FIA	Flow-injection Analysis
GC-MS	Gas Chromatography-Mass Spectrometry
HLA	Human Leukocyte Antigen
HPLC	High Performance Liquid Chromatography
IC	Ion Chromatography
IgA	Immunoglobulin A
IgG	Immunoglobulin G
IFN	Interferon
IR	Infrared
LCPL	Left Circularly Polarized Light
LOD	Limit of Detection
NIR	Near-infrared
OP	Organophosphate
PAR	4-(2-Pyridylazo) resorcinol
PDCA	Pyridine-2,6-dicarboxylic acid
PTH	Phenylthiohydantion
RCPL	Right Circularly Polarized Light
RSD	Relative Standard Deviation
THF	Tetrahydrofuran
TL	Thermal Lens
TLM	Thermal Lens Microscope
TLS	Thermal Lens Spectrometry
UV	Ultraviolet
Vis	Visible

RELATED ARTICLES

Infrared Spectroscopy of Biological Fluids in Clinical and Diagnostic Analysis
Infrared Spectroscopy of Biological Applications
Micro Total Analytical Systems in Clinical Chemistry
Laser- and Optical-based Techniques for the Detection of Explosives
Photoacoustic Spectroscopy in Trace Gas Monitoring
Infrared Spectroscopy in Environmental Analysis
Chemical-sensing Networks: Satellite-based
Near-infrared Spectroscopy in Food Analysis
Organophosphorus Pesticides in Water and Food, Analysis of
Coupled Liquid Chromatographic Techniques in Molecular Characterization
Multivariate Calibration of Analytical Data
Circular Dichroism and Linear Dichroism

REFERENCES

1. J.P. Gordon, R.C.C. Leite, R.S. Moore, S.P.S. Porto, J.R. Whinnery, 'Long-transient Effects in Lasers with Inserted Liquid Samples', *J. Appl. Phys.*, **36**, 3–8 (1965).
2. J.A. Sell, *Photothermal Investigations of Solids and Fluids*, Academic Press, New York, 1988.
3. D. Bicanic, *Photoacoustic and Photothermal Phenomena III*, Springer-Verlag, Berlin, 1992.
4. A. Mandelis, *Principles & Perpectives of Photothermal & Photoacoustic Phenomena*, Elsevier, New York, 1992.
5. C.D. Tran, 'Photothermal Detectors for High-performance Liquid Chromatography', in *HPLC Detection. Newer Methods*, ed. G. Patonay, VCH, New York, 111–126, 1992.
6. S.E. Bialkowski, *Photothermal Spectroscopy Methods for Chemical Analysis*, John Wiley & Sons, Inc., New York, 1996.
7. M. Franko, C.D. Tran, 'Analytical Thermal Lens Instrumentation', *Rev. Sci. Instrum.*, **67**, 1–18 (1996).
8. M. Franko, 'Thermal Lens Spectrometric Detection in Flow Injection Analysis and Separation Techniques', *Appl. Spectrosc. Rev.*, **43**, 358–388 (2008).
9. T. Kitamori, M. Tokeshi, A. Hibara, K. Sato, 'Thermal Lens Microscopy and Microchip Chemistry', *Anal. Chem.*, **76**, 52A–60A (2004).
10. A. Cognet, S. Berciaud, D. Lasne, B. Lounis, 'Photothermal Methods for Single Nonlumimescent Nano-objects', *Anal. Chem.*, **80**, 2289–2294 (2008).
11. H.C. Fang, R.L. Swoford, 'The Thermal Lens in Absorption Spectroscopy', in *Ultrasensitive Laser Spectroscopy*, ed. D.S. Kliger, Academic Press, 175–232, 1983.
12. N.J. Dovichi, 'Thermo-optical Spectrophotometries in Analytical Chemistry', *Crit. Rev. Anal. Chem.*, **17**, 357–423 (1987).
13. R. Gupta, 'Theory of Photothermal Effect in Fluids', in *Photothermal Investigations of Solids and Fluids*, ed. J.A. Sell, Academic Press, New York, 81–126, 1988.
14. J. Harris, 'Thermal Lens Effect', in *Analytical Applications of Lasers*, ed. E.H. Piepmeier, Wiley Interscience, New York, 451–554, 1986.

15. S.J. Sheldon, L.V. Knight, J.M. Thorne, 'Laser Induced Thermal Lens Effect: A New Theoretical Model', *Appl. Opt.*, **21**, 1663–1669 (1982).
16. J. Shen, R.D. Lowe, R.D. Snook, 'A Model for CW Laser Induced Mode-mismatched Dual-beam Thermal Lens Spectrometry', *Chem. Phys.*, **165**, 385–396 (1992).
17. M. Franko, C.D. Tran, 'Thermal Lens Technique for Sensitive Kinetic Determinations of Fast Chemical Reactions. Part I. Theory', *Rev. Sci. Instrum.*, **62**, 2430–2437 (1991).
18. M. Franko, C.D. Tran, 'Thermal Lens Technique for Sensitive Kinetic Determinations of Fast Chemical Reactions. Part II. Experiment', *Rev. Sci. Instrum.*, **62**, 2438–2442 (1991).
19. B. Li, S. Xiong, Y. Zhang, 'Fresnel Diffraction Model for Mode-mismatched Thermal Lens With Top-hat Beam Excitation', *Appl. Phys. B*, **80**, 527–534 (2005).
20. N.J. Dovichi, J.M. Harris, 'Laser Induced Thermal Lens Effect for Calorimetric Trace Analysis', *Anal. Chem.*, **51**, 728–731 (1979).
21. N.J. Dovichi, J.M. Harris, 'Time-resolved Thermal Lens Calorimetry', *Anal. Chem.*, **53**, 106–109 (1981).
22. T.-K.J. Pang, M.D. Morris, 'Liquid Chromatography Detection at the Second Harmonic of the Modulated Thermal Lens', *Anal. Chem.*, **56**, 1467–1469 (1984).
23. K.L. Jansen, J.M. Harris, 'Double-beam Thermal Lens Spectrometry', *Anal. Chem.*, **57**, 2434–2436 (1985).
24. K.J. Skogerboe, E.S. Yeung, 'Single Laser Thermal Lens Detector for Microbore Liquid Chromatography Based on High-frequency Modulation', *Anal. Chem.*, **58**, 1014–1018 (1986).
25. S.R. Erskine, C.M. Foley, D.R. Bobbitt, 'Single-laser, Single-Beam Pump/Probe Thermal Lens Spectroscopy', *Appl. Spectrosc.*, **41**, 1189–1193 (1987).
26. Y. Yang, 'Rotoreflected Laser Beam Thermal Lens Spectrometry', *Anal. Chem.*, **58**, 1420–1424 (1986).
27. T. Higashi, T. Imasaka, N. Ishibashi, 'Thermal Lens Spectrophotometry with Argon Laser Excitation Source for Nitrogen Dioxide Determination', *Anal. Chem.*, **55**, 1907–1910 (1983).
28. V.I. Grishko, C.D. Tran, W.W. Duley, 'Enhancement of the Thermal Lens Signal Induced by Sample Matrix Absorption of the Probe Laser Beam', *Appl. Opt.*, **41**, 5814–5822 (2002).
29. C.D. Tran, G. Huang, V.I. Grishko, 'Direct and Indirect Detection of Liquid Chromatography by Infrared Thermal Lens Spectrometry', *Anal. Chim. Acta*, **299**, 361–369 (1995).
30. M.S. Baptista, C.D. Tran, 'Near-infrared Thermal Lens Spectrometer Based on an Erbium-doped Fiber Amplifier and an Acousto-optic Tunable Filter, and Its Application in the Determination of Nucleotides', *Appl. Opt.*, **36**, 7059–7065 (1997).
31. N.J. Dovichi, J.M. Harris, 'Differential Thermal Lens Calorimetry', *Anal. Chem.*, **52**, 2338–2342 (1980).
32. T.-K.J. Pang, M.D. Morris, 'Differential Thermal Lens Liquid Chromatography Detector', *Anal. Chem.*, **57**, 2153–2155 (1985).
33. T. Berthoud, N. Delorme, 'Differential Dual-beam Thermal Lensing Spectrometry: Determination of Lanthanides', *Appl. Spectrosc.*, **41**, 15–19 (1987).
34. S.R. Erskine, D.R. Bobbit, 'Obliquely Crossed, Differential Thermal Lens Measurements Under Conditions of High Background Absorbance', *Appl. Spectrosc.*, **43**, 668–674 (1989).
35. M. Franko, D. Bicanic, 'Differential Thermal Lens Spectroscopy in the Infrared', *Isr. J. Chem.*, **38**, 175–179 (1998).
36. M. Franko, C.D. Tran, 'Development of a Double-beam, Dual-wavelength Thermal-lens Spectrometer for Simultaneous Measurement of Absorption at Two Different Wavelengths', *Anal. Chem.*, **60**, 1925–1928 (1988).
37. C.D. Tran, M. Xu, 'Dual-wavelength Photothermal Refraction Spectrometry for Small-volume Samples', *Appl. Spectrosc.*, **43**, 1056–1061 (1989).
38. C.W. Earle, N.J. Dovichi, 'Simultaneous Two-color Two-laser Beam Thermo-optical Absorbance Detector for Capillary Zone Electrophoresis', *J. Liq. Chromatogr.*, **12**, 2575–2585 (1989).
39. M. Xu, C.D. Tran, 'Multi-wavelength Thermal Lens Spectrophotometer', *Anal. Chim. Acta*, **235**, 445–449 (1990).
40. C.D. Tran, V. Simianu, 'Multiwavelength Thermal Lens Spectrophotometer Based on an Acousto-optic Tunable Filter', *Anal. Chem.*, **64**, 1419–1425 (1992).
41. C.D. Tran, M. Xu, 'Ultrasensitive Thermal Lens-circular Dichroism Spectropolarimeter for Small-volume Samples', *Rev. Sci. Instrum.*, **60**, 3207–3211 (1989).
42. M. Xu, C.D. Tran, 'Thermal Lens-circular Dichroism Spectropolarimeter', *Appl. Spectrosc.*, **44**, 962–966 (1990).
43. M. Xu, C.D. Tran, 'Thermal Lens-circular Dichroism Detector for High-performance Liquid Chromatography', *Anal. Chem.*, **62**, 2467–2471 (1990).
44. G.R. Long, S.E. Bialkowski, 'Pulsed Infrared Laser Thermal Lens Spectrophotometric Determination of Trace-level Gas-phase Analytes: Quantitation of Parts Per Billion Dichlorodifluoromethane', *Anal. Chem.*, **56**, 2806–2811 (1984).
45. S.E. Bialkowski, 'Pulsed Laser Thermal Lens Spectrophotometry of Liquid Samples Using an Optical

Fiber Beam Guide with Interference Orthogonal Signal Processing', *Anal. Chem.*, **58**, 1706–1710 (1986).

46. T. Imasaka, K. Nakanishi, N. Ishibashi, 'A Couple of Optical Fibers for Thermal Lens Spectrophotometry', *Anal. Chem.*, **59**, 1554–1557 (1987).
47. D. Rojas, R.J. Silva, J.D. Spear, R.E. Russo, 'Dual-beam Optical Fiber Thermal Lens Spectroscopy', *Anal. Chem.*, **63**, 1927–1932 (1991).
48. K. Nakanishi, T. Imasaka, N. Ishibashi, 'Thermal Lens Spectrophotometry of Phosphorus Using a Near-infrared Semiconductor Laser', *Anal. Chem.*, **57**, 1219–1223 (1985).
49. E. Tamaki, A. Hibara, M. Tokeshi, T. Kitamori, 'Microchannel-Asssisted Thermal-lens Spectrometry for Microchip Analysis', *J. Chromatogr., A*, **987**, 197–204 (2003).
50. A. Chartier, S.E. Bialkowski, 'Photothermal Spectrometry in Small Liquid Channels', *Anal. Sci.*, **17**, i99–i101 (2002).
51. T. de Beer, N.H. Velthorst, U.A.T. Brinkman, C. Gooijer, 'Laser-Based Non-fluorescence Detection Techniques for Liquid Separation Systems', *J. Chromatogr., A*, **971**, 1–35 (2002).
52. D. Bicanic, M. Franko, J. Gibkes, E. Gerkema, J.P. Favier, H. Jalink, 'Applications of Photoacoustic and Photothermal Non-contact Methods in the Selected Areas of Environmental and Agricultural Sciences', in *Progress in Photothermal and Photoacoustic Science and Technology, Vol. 3, Life and Earth Sciences*, ed. A. Mandelis, SPIE-Optical Engineering Press, Bellingham, 131–180, 1996.
53. M. Šikovec, M. Franko, F.G. Cruz, S.A. Katz, 'Thermal Lens Spectrometric Determination of Hexavalent Chromium', *Anal. Chim. Acta*, **330**, 245–250 (1996).
54. A. Madžgalj, M.L. Baesso, M. Franko, 'Flow Injection – Thermal Lens Spectrometric Determination of Hexavalent Chromium', *Eur. Phys. J. Special Topics*, **153**, 503–506 (2008).
55. B. Divjak, M. Franko, Mi. Novič, 'Determination of Iron Complex Matrices by Ion Chromatography With UV-Vis, Thermal Lens and Amperometric Detection Using Post-Column Reagents', *J. Chromatogr., A*, **829**, 167–174 (1998).
56. M. Šikovec, M. Novič, V. Hudnik, M. Franko, 'On-line Thermal Lens Spectrometric Detection of Cr(III) and Cr(VI) After Separation by Ion Chromatography', *J. Chromatogr., A*, **706**, 121–126 (1995).
57. M. Šikovec, M. Franko, M. Novič, M. Veber, 'Effect of Organic Solvents in the On-line Thermal Lens Spectrometric Detection Of Chromium(III) and Chromium(VI) After Ion Chromatographic Separation', *J. Chromatogr. A*, **920**, 119–125 (2001).
58. M. Šikovec, M. Novič, M. Franko, 'Application of Thermal Lens Spectrometric Detection to the Determination of Heavy Metals by Ion Chromatography', *J. Chromatogr., A*, **739**, 111–117 (1996).
59. B.S. Seidel, W. Faubel, 'Miniaturized Capillary Electrophoretic Drug Analysis with Photothermal Detection', in *Photoacoustic and Photothermal Phenomena, 10th International Conference*, eds. F. Scudieri, M. Bertolotti, American Institute of Physics, 576–578, 1999.
60. V. Guzsvány, A. Madžgalj, P. Trebše, F. Gaál, M. Franko, 'Determination of Some Neonicotinoid Insecticides by Liquid Chromatography with Thermal Lens Spectrometric Detection', *Environ. Chem. Lett.*, **5**, 203–208 (2007).
61. L. Pogačnik, M. Franko, 'Determination of Organophosphate and Carbamate Pesticides in Vegetable Samples by a Photothermal Biosensor', *Biosens. Bioelectron.*, **18**, 1–9 (2003).
62. M. Bavcon-Kralj, P. Trebše, M. Franko, 'Applications of Bioanalytical Techniques in Evaluating Advanced Oxidation Processes in Pesticide Degradation', *Trends Anal. Chem.*, **26**, 1020–1031 (2007).
63. M. Bavcon-Kralj, M. Franko, P. Trebše, 'Photodegradation of Organophosphorous Insecticides – Investigation of Products and Their Toxicity Using Gas Chromatography-mass Spectrometry and AChE-thermal Lens Spectrometric Bioassay', *Chemosphere*, **67**, 99–107 (2007).
64. M. Bavcon-Kralj, U. Černigoj, M. Franko, P. Trebše, 'Comparison of Photocatalysis and Photolysis of Malathion, Isomalathion, Malaoxon, and Commercial Malathion-products and Toxicity Studies', *Water Res.*, **41**, 4504–4514 (2007).
65. J. Kožar-Logar, A. Malej, M. Franko, 'Double Dual Beam Thermal Lens Spectrometer for Monitoring of Phytoplankton Cell Lysis', *Instrum. Sci. Technol.*, **34**, 23–31 (2006).
66. J. Kožar Logar, A. Malej, M. Franko, 'Hyphenated High Performance Liquid Chromatography-thermal Lens Spectrometry Technique as a Tool for Investigations of Xanthophyll Cycle Pigments in Different Taxonomic Groups of Marine Phytoplankton', *Rev. Sci. Instrum.*, **74**, 776–778 (2003).
67. M. Franko, D. Bicanic, J. Gibkes, M. Bremer, E. Akkermans, 'Thermal Lens Spectrometric Detection and Characterization of Fatty Acids', *Food Technol. Biotechnol.*, **35**, 39–43 (1997).
68. A. Cladera Forteza, C. Tomas Mas, J.M. Estela Ripoll, V. Cerda Martin, G. Ramis-Ramos, 'Determination of Tannins in White Wines by Thermal Lens Spectrometry', *Microchem. J.*, **52**, 28–32 (1995).

69. M. Franko, 'Recent Applications of Thermal Lens Spectrometry in Food Analysis and Environmental Research', *Talanta*, **54**, 1–13 (2001).

70. S. Luterotti, M. Franko, M. Šikovec, D. Bicanic, 'Ultrasensitive Assays of Trans- and cis-β-carotenes in Vegetable Oils by High-performance Liquid Chromatography-thermal Lens Detection', *Anal. Chim. Acta*, **460**, 193–200 (2002).

71. S. Luterotti, M. Franko, D. Bicanic, 'Fast Quality Screening of Vegetable Oils by HPLC-thermal Lens Spectrometric Detection', *J. Am. Oil Chem. Soc.*, **79**, 1027–1031 (2002).

72. D. Bicanic, O. Doka, S. Luterotti, A. Bohren, M. Šikovec, B. van Veldhuizen, O. Berkessy, M. Chirtoc, M. Franko, G. Szabo, M. Sigrist, 'Assessing the Extent of Oxidation in Thermally Stressed Vegetable Oils. Part I: Optical Characterization by Photothermal and Some Conventional Physical Methods', *Anal. Sci.*, **17**, S547–S550 (2001).

73. S. Luterotti, K. Markovič, M. Franko, D. Bicanic, N. Vahčić, O. Doka, 'Ultratraces of Carotenes in Tomato Purees: HPLC – TLS Study', *Rev. Sci. Instrum.*, **74**, 684–686 (2003).

74. M. Franko, M. Šikovec, J. Kožar-Logar, D. Bicanic, 'Thermal Lens Spectrometry in Food Analysis and Environmental Research', *Anal. Sci.*, **17**, S515–S518 (2001).

75. V. Zharov, V. Galitovskiy, C.S. Lyle, T.C. Chambers, 'Superhigh-sensitivity Photothermal Monitoring of Individual Cell Response to Antitumor Drug', *J. Biomed. Opt.*, **11**, 064034/1–064034/11 (2006).

76. V. Zharov, E. Galanzha, V.V. Tuchin, 'In Vivo Photothermal Flow Cytometry: Imaging and Detection of Individual Cells in Blood and Lymph Flow', *J. Cell. Biochem.*, **97**, 916–932 (2006).

77. H. Kimura, F. Nagao, A. Kitamura, K. Sekiguchi, T. Katamori, T. Sawada, 'Detection and Measurement of a Single Blood Cell Surface Antigen by Thermal Lens Miscroscopy', *Anal. Chim. Acta*, **283**, 27–32 (2000).

78. M. Harada, K. Iwamoto, T. Kitamori, T. Sawada, 'Photothermal Microscopy with Excitation and Probe Beams Coaxial under the Microscope and its Application to Microparticle Analysis', *Anal. Chem.*, **65**, 2938–2940 (1993).

79. M. Harada, M. Shibata, T. Kitamori, T. Sawada, 'Application of Coaxial Beam Photothermal Microscopy to the Analysis of a Single Biological Cell in Water', *Anal. Chim. Acta*, **299**, 343–347 (1995).

80. H. Kimura, K. Sekiguchi, T. Kitamori, T. Sawada, M. Mukaida, 'Assay of Spherical Cell Surface Molecules by Thermal Lens Microscopy and its Application to Blood Cell Substances', *Anal. Chem.*, **73**, 4333–4337 (2001).

81. M. Harada, M. Masashi, T. Kitamori, T. Sawada, 'Sub-attomole Molecule Detection in a Single Biological Cell In-vitro by Thermal Lens Microscopy', *Anal. Sci.*, **15**, 647–650 (1999).

82. H. Kimura, F. Nagao, A. Kitamura, K. Sekiguchi, T. Takehiko, T. Sawada, 'Detection and Measurement of a Single Blood Cell Surface Antigen by Thermal Lens Microscopy', *Anal. Biochem.*, **283**, 27–32 (2000).

83. H. Kimura, H. Kojima, M. Mukaida, T. Kitamori, T. Sawada, 'Analysis of Serum Proteins Adsorbed to a Hemodialysis Membrane of Hollow Fiber Type by Thermal Lens Microscopy', *Anal. Sci.*, **15**, 1101–1107 (1999).

84. H. Kimura, T. Kitamori, T. Sawada, 'Critical Increment of Lewis Blood Group Antigen in Serum by Cancer Found by Photothermal Immunoassay', *Anal. Biochem.*, **274**, 98–103 (1999).

85. H. Kimura, M. Mukaida, T. Kitamori, T. Sawada, 'Quantitation of Drug Concentration by Photo-thermal Microscopy in a Renal Tubule of Fixed Kidney', *Anal. Sci.*, **13**, 729–734 (1997).

86. K. Sato, M. Yamanaka, T. Hagino, M. Tokeshi, H. Kimura, T. Kitamori, 'Microchip-based Enzyme-Linked Immunosorbent Assay (Microelisa) System with Thermal Lens Detection', *Lab Chip*, **4**, 570–575 (2004).

87. H. Sorouraddin, H. Hibara, T. Kitamori, 'Use of a Thermal Lens Microscope in Integrated Catecholamine Determination on a Microchip', *Fresenius' J. Anal. Chem.*, **371**, 91–96 (2001).

88. E. Tamaki, K. Sato, M. Tokeshi, K. Sato, M. Aihara, T. Kitamori, 'Single-cell Analysis by a Scanning Thermal Lens Microscope With a Microchip: Direct Monitoring of Cytochrome C Distribution During Apoptosis Process', *Anal. Chem.*, **74**, 1560–1564 (2002).

89. K. Sato, M. Tokeshi, H. Kimura, T. Kitamori, 'Determination of Carcinoembryonic Antigen in Human Sera by Integrated Bead-bed Immunoassay in a Microchip for Cancer Diagnosis', *Anal. Chem.*, **73**, 1213–1218 (2001).

90. C.D. Tran, V.I. Grishko, 'Thermal Lens Technique for Sensitive and Nondestructive Determination of Isotopic Purity', *Anal. Biochem.*, **218**, 197–203 (1994).

91. C.D. Tran, V.I. Grishko, 'Measuring Infrared Absorption in the Visible: Sensitive Determinations of Chemical and Isotopic Purity of Solvents by Thermal Lens Effect', *Appl. Spectrosc.*, **48**, 96–100 (1994).

92. C.D. Tran, V.I. Grishko, M.S. Baptista, 'Nondestructive and Nonintrusive Determination of Chemical and Isotopic Purity of Solvents by Near-infrared Thermal Lens Spectrometry', *Appl. Spectrosc.*, **48**, 833–842 (1994).

93. M. Baptista, C.D. Tran, 'Near - Infrared Thermal Lens Spectrometer Based on an Erbium-doped Fiber Amplifier and an Acousto-optic Tunable Filter, and its Application

in the Determination of Nucleotides', *Appl. Opt.*, **36**, 7059–7065 (1997).

94. Y. Dwivedi, S.B. Rai, 'Spectroscopic Study of Overtone and Combination Bands in Aliphatic Aldehydes', *Vib. Spectrosc.*, **49**, 278–283 (2009).
95. A. Lopez-Calvo, C.E. Manzanares, 'Overtone Spectroscopy and Thermal Lens Detection Limit of Methane in Cryo-Solutions', *Mol. Phys.*, **106**, 909–920 (2008).
96. A. Lopez-Calvo, C.E. Manzanares, 'Thermal Lens Spectroscopy in Cryogenic Solutions: Analysis and Comparison of Intensities in CH_4-N_2 and CH_4-Ar Liquid Solutions', *J. Phys. Chem. A*, **110**, 10427–10434 (2006).
97. J.G. Navea, A. Lopez-Calvo, C.E. Manzanares, 'Thermal Lens Spectroscopy in Liquid Argon Solutions: ($\Delta v = 6$) C-H Vibrational Overtone Absorption of Methane', *J. Phys. Chem. A*, **110**, 1594–1599 (2006).
98. A. Lopez-Calvo, C.E. Manzanares, 'Vibrational Overtone Spectroscopy of Saturated Hydrocarbons Dissolved in Liquefied Ar, Kr, Xe, and N_2', *J. Phys. Chem. A*, **112**, 1730–1740 (2008).
99. J. Amador-Hernandez, J.M. Fernandez-Romero, M.D. Luque de Castro, 'Near Infrared Thermal Lens Spectrometry for The Real-time Monitoring of Supercritical Fluid Extraction', *Talanta*, **49**, 813–823 (1999).
100. T.M.A. Rasheed, 'C-H Overtone Spectrum of Biphenyl-evidence for the Cumulative Effect of Conjugated Resonance Structures', *Spectrochim. Acta, Part A*, **52A**, 1493–1497 (1996).
101. J.V. Prasad, S.B. Rai, 'Overtone Spectroscopy of Methyl, Ethyl Alcohols And Cyanides', *Indian J. Phys., B*, **69B**, 471–476 (1995).
102. J.V. Prasad, I.B. Singh, S.B. Rai, S.N. Thakur, 'Overtone Spectroscopy of Aniline and Haloanilines', *Indian J. Phys., B*, **69B**, 315–322 (1995).
103. T.M. Abdul Rasheed, K.P.B. Moosad, V.P.N. Nampoori, K. Sathianandan, 'Carbon-hydrogen Local Mode Excitations and Fermi Resonance in Trichloroethylene', *Spectrochim. Acta, Part A*, **43A**, 1183–1186 (1987).
104. T.M. Abdul Rasheed, K.P.B. Moosad, V.P.N. Nampoori, K. Sathianandan, 'C-H Overtones in Acetophenone and Benzaldehyde: Aryl and Methyl Local Modes', *J. Phys. Chem.*, **91**, 4228–42231 (1987).
105. Y. Mizugai, M. Katayama, M. Nakagawa, 'Substituent Effect on the Fifth Overtones of the Aryl Carbon-hydrogen Stretching Vibrations in Disubstituted Benzenes', *J. Am. Chem. Soc.*, **103**, 5061–5063 (1981).
106. Y. Mizugai, F. Takimoto, M. Katayama, 'The Fourth Overtone of the Free Oxygen-hydrogen Stretching Vibrations of Alcohols and Their Solvent Effect', *Chem. Phys. Lett.*, **76**, 615–618 (1980).
107. Y. Mizugai, M. Katayama, 'The Fifth Overtones of the Carbon-hydrogen Stretching Vibrations and the Bond Lengths in Some Heterocyclic Compounds', *Chem. Phys. Lett.*, **73**, 240–243 (1980).
108. P.R.B. Pedreira, L.R. Hirsch, J.R.D. Pereira, A.N. Medina, A.C. Bento, M.L. Baesso, M.C.E. Rollemberg, M. Franko, 'Observation of Laser Induced Photochemical Reaction of Cr(VI) Species in Water During Thermal Lens Measurements', *Chem. Phys. Lett.*, **396**, 221–225 (2004).
109. P.R.B. Pedreira, L.R. Hirsch, J.R.D. Pereira, A.N. Medina, A.C. Bento, M.L. Baesso, M.C.E. Rollemberg, M. Franko, J. Shen, 'Real-time Quantitative Investigation of Photochemical Reaction Using Thermal Lens Measurements: Theory and Experiment', *J. Appl. Phys.*, **100**, 044906 (2006).
110. M. Terazima, 'Refractive Index Change by Photothermal Effect with a Constant Density Detected as Temperature Grating in Various fluids', *J. Chem. Phys.*, **104**, 4988–4998 (1996).
111. M. Harada, K. Iwamoto, T. Kitamori, T. Sawada, 'Photothermal Microscopy with Excitation and Probe Beams Coaxial Under the Microscope and its Application to Microparticle Analysis', *Anal. Chem.*, **65**, 2938–2940 (1993).
112. K. Sato, M. Tokeshi, T. Kitamori, T. Sawada, 'Integration of Flow Injection Analysis and Zeptomole-level Detection of the Fe(II)-o-phenanthroline Complex', *Anal. Sci.*, **15**, 641–645 (1999).
113. M.A. Proskurnin, M.N. Slyadnev, M. Tokeshi, T. Kitamori, 'Optimization of Thermal Lens Microscopic Measurements in a Microchip', *Anal. Chim. Acta*, **480**, 97–95 (2003).
114. H.M. Sorouraddin, A. Hibara, M.A. Proskrunin, T. Kitamori, 'Integrated FIA for the Determination of Ascorbic Acid and Dehydroascorbic Acid in a Microfabricated Glass-channel by Thermal-lens Microscopy', *Anal. Sci.*, **16**, 1033–1037 (2000).
115. H.M. Sorouraddin, A. Hibara, T. Kitamori, 'Use of a Thermal Lens Microscope in Integrated Catecholamine Determination on a Microchip', *Fresenius' J. Anal. Chem.*, **371**, 91–96 (2001).
116. H. Hotokezaka, M. Tokeshi, M. Harada, T. Kitamori, Y. Ikeda, 'Development of the Innovative Nuclide Separation System for High-level Radioactive Waste Using Microchannel Chip - Extraction Behavior of Metal Ions from Aqueous Phase to Organic Phase in Microchannel', *Prog. Nucl. Energy*, **47**, 439–447 (2005).
117. M. Tokeshi, M. Uchida, A. Hibara, T. Sawada, T. Kitamori, 'Determination of Sub-yoctomole Amounts of Non-fluorescent Molecules Using a Thermal Lens Microscope: Sub-single Molecule Determination', *Anal. Chem.*, **73**, 2112–2116 (2001).
118. M. Tokeshi, T. Minagawa, T. Kitamori, 'Integration of a Microextraction System on a Glass Chip:

Ion-pair Solvent Extraction of Fe(II) with 4,7-diphenyl-1,10-phenanthrolinedisulfonic Acid and Tri-N-octylmethylammonium Chloride', *Anal. Chem.*, **72**, 1711–1714 (2000).

119. H. Hisamoto, T. Horiuchi, M. Tokeshi, A. Hibara, T. Kitamori, 'On-chip Integration of Neutral Ionophore-based Ion Pair Extraction Reaction', *Anal. Chem.*, **73**, 1382–1386 (2001).
120. M. Tokeshi, T. Minagawa, K. Uchiyama, A. Hibara, K. Sato, H. Hisamoto, T. Kitamori, 'Continuous Flow Chemical Processing on a Microchip by Combining Micro Unit Operations and a Multiphase Flow Network', *Anal. Chem.*, **74**, 1565–1571 (2002).
121. A. Smirnova, K. Shimura, A. Hibara, M.A. Proskurnin, T. Kitamori, 'Application of a Micro Multiphase Laminar Flow on a Microchip for Extraction and Determination of Derivatized Carbamate Pesticides', *Anal. Sci.*, **23**, 103–107 (2007).
122. K. Sato, A. Egami, T. Odake, M. Tokeshi, M. Aihara, T. Kitamori, 'Monitoring of Intercellular Messengers Released from Neuron Networks Cultured in a Microchip', *J. Chromatogr., A*, **1111**, 228–232 (2006).
123. K. Sato, M. Tokeshi, T. Odake, H. Kimura, T. Ooi, M. Nakao, T. Kitamori, 'Integration of an Immunosorbent Assay System: Analysis of Secretory Human Immunoglobulin A on Polystyrene Beads in a Microchip', *Anal. Chem.*, **72**, 1144–1147 (2000).
124. M.A. Proskurnin, S.N. Bendrysheva, N. Ragozina, S. Heissler, W. Faubel, U. Pyell, 'Optimization of Instrumental Parameters of a Near-field Thermal-lens Detector for Capillary Electrophoresis', *Appl. Spectrosc.*, **59**, 1470–1479 (2005).
125. K. Uchiyama, M. Tokeshi, Y. Kikutani, A. Hattori, T. Kitamori, 'Optimization of an Interface Chip for Coupling Capillary Electrophoresis with Thermal Lens Microscopic Detection', *Anal. Sci.*, **21**, 49–52 (2005).
126. B.S. Seidel, W. Faubel, 'Fiber Optic Modified Thermal Lens Detector System for the Determination of Amino Acids', *J. Chromatogr., A*, **817**, 223–226 (1998).
127. Y. Hu, J. Cheng, Y. Deng, 'On-Column Indirect Photothermal Interference Detection for Capillary Zone Electrophoresis', *Analyst*, **122**, 1089–1093 (1997).
128. J. Ren, B. Li, Y. Deng, J. Cheng, 'Indirect Thermo-optical Detection for Capillary Electrophoresis', *Talanta*, **42**, 1891–1895 (1995).
129. M. Qi, X.F. Li, C. Stathakis, N.J. Dovichi, 'Capillary Electrochromatography with Thermo-optical Absorbance Detection for the Analysis of Phenylthiohydantoin-amino Acids', *J. Chromatogr., A*, **853**, 131–140 (1999).
130. X.F. Li, S.J. Carter, N.J. Dovichi, 'Non-aqueous Capillary Electrophoresis of Tamoxifen and its Acid Hydrolysis Products', *J. Chromatogr., A*, **895**, 81–85 (2000).
131. N.Y. Ragozina, M. Pütz, S. Heissler, W. Faubel, U. Pyell, 'Quantiffication of Etoposide and Etoposide Phosphate in Human Plasma by Micellar Electrokinetic Chromatography and Near Field Thermal Lens Detection', *Anal. Chem.*, **76**, 3804–3809 (2004).
132. D.A. Nedosekin, S.N. Bendrysheva, W. Faubel, M.A. Proskurnin, U. Pyell, 'Indirect Thermal Lens Detection for Capillary Electrophoresis', *Talanta*, **71**, 1788–1794 (2007).
133. B.S. Seidel, W. Faubel, 'Determination of Iron in Real Samples by High Performance Capillary Electrophoresis in Combination with Thermal Lensing', *Fresenius' J. Anal. Chem.*, **360**, 795–797 (1998).
134. C.D. Tran, 'Simultaneous Enhancement of Fluorescence and Thermal Lensing by Reversed Micelles', *Anal. Chem.*, **60**, 182–185 (1988).
135. M. Franko, C.D. Tran, 'Temperature Effect on Photothermal Lens Phenomena in Water: Photothermal Focusing and Defocusing', *Chem. Phys. Lett.*, **158**, 31–36 (1989).
136. M. Franko, C.D. Tran, 'Water as a Unique Medium for Thermal Lens Measurements', *Anal. Chem.*, **61**, 1660–1666 (1989).
137. S.E. Braslavski, G.E. Heibel, 'Time-Resolved Photothermal and Photoacoustic Methods Applied to Photoinduced Processes in Solution', *Chem. Rev.*, **96**, 1381–1410 (1992).
138. M. Terazima, 'Refractive Index Change by Photothermal Effect with a Constant Density Detected as Temperature Grating in Various Fluids', *J. Chem. Phys.*, **104**, 4988–4998 (1996).
139. M. Franko, C.D. Tran, 'Thermal Lens Effect in Electrolyte and Surfactant Media', *J. Phys. Chem.*, **95**, 6688–6696 (1991).
140. M.S. Baptista, C.D. Tran, 'Structural Investigation of the Effects of Nonelectrolytes and Surfactants on Water by Thermal Lens Spectrometry', *J. Phys. Chem.*, **99**, 12952–12961 (1995).
141. M.S. Baptista, C.D. Tran, 'Electrical Conductivity, Near Infrared Absorption and Thermal Lens Spectroscopic Studies of Percolation of Microemulsions', *J. Phys. Chem., B*, **101**, 4209–4217 (1997).
142. C.D. Tran, T.A. Van Fleet, 'Micellar Induced Simultaneous Enhancement of Fluorescence and Thermal Lensing', *Anal. Chem.*, **60**, 2478–2482 (1988).
143. C.D. Tran, W. Zhang, 'Thermal Lensing Detection of Lanthanide Ions by Solvent Extraction Using Crown Ethers', *Anal. Chem.*, **62**, 830–834 (1990).
144. C.D. Tran, 'Ionic Liquids for and by Analytical Chemistry', *Anal. Lett.*, **40**, 2447–2464 (2007).
145. C.D. Tran, S. Challa, M. Franko, 'Ionic Liquids as an Attractive Alternative Solvent for Thermal Lens Measurements', *Anal. Chem.*, **77**, 7442–7447 (2005).

146. A. Bjarkley, *Optical Fiber Amplifiers: Design and System Applications*, Artech House, Boston, MA, 1993.

147. E. Desurvire, *Erbium Doped Fiber Amplifiers*, Wiley, New York, 1994.

148. T.A. Alexander, G.H. Gao, C.D. Tran, 'Development of a Novel Fluorimeter Based on Superliminescent Light Emitting Diodes and an Acousto-optical Tunable Filter and its Application in the Determination of Chlorophyll a and b', *Appl. Spectrosc.*, **51**, 1603–1606 (1997).